

國立臺灣大學理學院大氣科學研究所

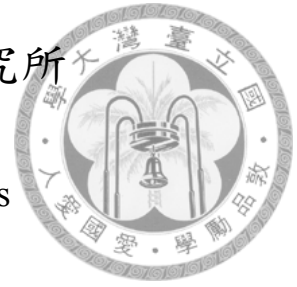
碩士論文

Graduate Institute of Atmospheric Sciences

College of Science

National Taiwan University

Master Thesis



農業灌溉於低緯度地區造成之冬季時期高土壤濕度對區域與
全球氣候之可能影響

Potential Impacts of Wintertime Soil Moisture Anomalies from
Agricultural Irrigation at Low Latitudes on Regional and Global
Climate

魏豪緯

Hao-wei Wey

指導教授：羅敏輝博士

Advisor: Min-Hui Lo, Ph.D.

中華民國 104 年 6 月

June, 2015

國立臺灣大學碩士學位論文 口試委員會審定書

本論文係 魏豪緯 君 (學號 R02229011) 在國立臺灣大學大氣科學學系、所完成之碩士學位論文，於民國 104 年 6 月 12 日承下列考試委員審查通過及口試及格，特此證明

口試委員：

羅劍輝

(簽名)

(指導教授)

李時雨

陳維婷

黃彥婷

張宇

系主任、所長

理學院大氣
科學系系主任 林依依

(簽名)



致謝

那個時候我們像螻蛄一樣地站在海邊。血紅色的夕陽落入海平面，浪頭啪嗒啪嗒一波一波襲來，偏執地像要抓住誰的腳。靜極，除此之外再無其它。

然後，界限突然如此清晰地模糊起來：關於沙灘，關於海，關於天空，也關於我背後的沒落小鎮以及那些小得只能是點，成對或形單影隻而面容不明的人們。

我下了很大的決心回來。告訴自己，應該記得那一刻，無論我們選擇用什麼方式描述這個世界。

感謝指導教授羅敏輝老師這兩年多來的耐心指導，讓我可以順利完成論文與研究，老師的研究熱情和科學精神更是我的努力目標。感謝口試委員陳維婷老師、王世宇老師、李時雨老師和黃彥婷老師的寶貴意見，讓這篇論文可以更加完整。感謝陳維婷老師和吳健銘老師在實驗室的聯合會議時提出的許多一針見血的問題，讓我的思考不要太過侷限。感謝大氣系和大氣系以外所有熱心地給予我關心與幫助的老師們，不管是知識上、生活上甚至是為人處事，我總是從老師們的身上學到許多。感謝大氣系的學長姊、同學、助理和每一位實驗室夥伴，謝謝你們在各方面的幫忙，到後來我也發現了，C404 不只看起來很像網咖，其實也是很歡樂的。

謝謝出，謝謝你講笑話給我聽，以及所有你為我做的事。

最後，要感謝我的家人們，沒有你們毫無保留的支持與陪伴就不會有這一篇論文。



中文摘要

了解農業灌溉對環境造成的影響一直都是重要的課題。人為的水資源管理（如灌溉）足以改變地表的能量收支與水循環。在本研究中，我們關注在亞洲低緯度地區的灌溉行為對冬季時期區域和全球氣候的可能影響。我們利用地球系統模式模擬陸地與大氣交互作用如何受到灌溉的影響，以及大氣環流如何改變。我們發現，不考慮灌溉的模式模擬低估了冬季在印度河—恆河平原的平均蒸發散量。比較有無考慮灌溉的模式模擬結果顯示，低緯度地區的灌溉使得冬季時期有較高的土壤濕度，從而降低了地表鮑文比，經由大氣的迴饋造成整個印度次大陸尺度的地表降溫。由於較大的海陸熱力差異，盛行季風亦有所增強。此外，熱帶地區的降水與中緯度的氣候皆有改變，顯示了熱帶與溫帶間的遙相關關係。冬季的阿留申低壓加深並向東移動，儘管在冬季，北美幾乎沒有進行任何灌溉，但實驗中在北美陸地則有增暖的現象。在前人的研究中曾發現此增暖現象，但並無加以解釋，因此本研究提供了一個合理的機制，亦即此北美的增暖現象是來自於在亞洲低緯度地區進行灌溉所造成的影響。

關鍵字：灌溉、陸地—大氣交互作用、印度河—恆河平原、熱帶—溫帶遙相關、阿留申低壓

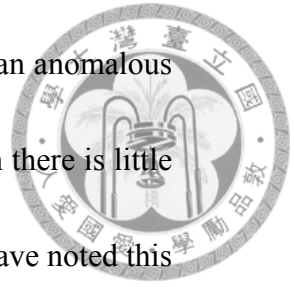


Abstract

The effect of agricultural irrigation on the environment has long been a critical concern. Anthropogenic water management can change surface-energy budgets and the water cycle. In this study, we focused on the impacts of Asian low-latitude irrigation on regional and global climates during boreal wintertime. We used a state-of-the-art earth system model to simulate land–air interaction processes affected by water management and the consequent responses in atmospheric circulation. Modeling without considering irrigation underestimates evapotranspiration in the Indo-Gangetic Plain during winter. Perturbed experiments show that wet-soil-moisture anomalies at low latitudes can lower the surface Bowen ratio and reduce the surface temperature to a continental scale through atmospheric feedback. The intensity of prevailing monsoon circulation becomes stronger because of larger land–sea thermal contrast. In addition, anomalous tropical precipitation and mid-latitude climatic changes indicate tropical–extratropical teleconnections. The

wintertime Aleutian low is deepened and shifts eastward, and an anomalous warm surface temperature is found in North America, although there is little irrigation over North America in the winter. Previous studies have noted this warming but left it unexplained, and we provide a plausible mechanism for these remote impacts, which come from the irrigation over Asian low-latitude regions.

Key words: irrigation, land-air interaction, Indo-Gangetic Plain, tropical-extratropical teleconnection, Aleutian low





Contents

口試委員會審定書	i
致謝	ii
中文摘要	iii
Abstract	iv
Contents	vi
List of Figures	viii
List of Tables	xi
1 Introduction	1
2 Methodology	5
2.1 Data sets	5
2.2 Model setup	6

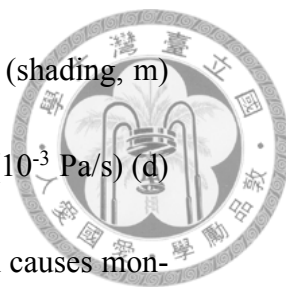


3 Results	8
3.1 Regional impacts induced by the irrigation over the Indo-Gangetic Plain	8
3.2 Remote impacts on the North American winter climate	12
4 Discussion	16
4.1 Remote impacts of winter monsoon variability	16
4.2 Memory effects of soil moisture anomalies	19
4.3 Teleconnection without tropical influences	20
5 Conclusion	22
5.1 Summary	22
5.2 Future works	23
5.2.1 Influences of moisture supply from irrigation to fog formation	24
5.2.2 Irrigation in West Asia impacts to glacier status in Tibetan Plateau and surroundings	25
5.2.3 Cross basin influences of Indian Ocean	26
Bibliography	29



List of Figures

2.1	Hydrology processes simulated in CLM4. Taken from CLM4 tech note (Oleson et al., 2010).	42
2.2	Global annual mean irrigation added in the simulation (mm/year)	43
3.1	(a) January-March mean irrigation amount (mm/month). The location of IGP is also shown. (b) Climatological means of AVHRR and FLUXNET based ET, irrigation amount and PET averaged over IGP (mm/month). (c) Simulated IGP mean ET from CESM compared with the two observation products (W/m ²).	44
3.2	The water cycle. Taken from UNEP (2008)	45
3.3	CESM temperature bias in JFM compared with CRU record (K)	45
3.4	IRR-CTR (a) 10cm soil water (kg/m ²) (b) latent heat flux (W/m ²) (c) low cloud cover (d) surface downwelling shortwave flux (W/m ²) and (e) reference height temperature (K). (dotted: $p < 0.1$)	46



3.5	IRR-CTR (a) 925-hPa and (b) 200-hPa geopotential height (shading, m) and wind (vector, m/s) (c) 40E-90E mean vertical velocity (10^{-3} Pa/s) (d) Schematic diagram showing the process of which irrigation causes monsoon changes (e) IRR-CTR 200-hPa velocity potential (10^5 m ² /s) (dotted: $p < 0.1$ for a, b, and e)	47
3.6	(a) zonal mean meridional stream function (shading: IRR-CTR, 10^9 kg/s; contour: CTR, CI: 0.2×10^{11} kg/s, positive (negative) values are in solid (dashed) lines) (b) IRR-CTR 200-hPa zonal wind (m/s) (c) IRR-CTR sea level pressure (Pa) (dotted: $p < 0.1$ for b and c)	48
3.7	IRR-CTR total precipitation rate (mm/day) (dotted: $p < 0.1$)	49
3.8	IRR-CTR (red) and CTR (black) zonal mean precipitation (mm/day) . . .	49
3.9	Differences (IRR-CTR) in (a) 500-hPa geopotential height (m); (b) reference height temperature over North America (K) (dotted: $p < 0.1$).	50
4.1	Composite 200-hPa zonal wind difference (ERA-Interim reanalysis) (m/s)	51
4.2	Composite 200-hPa zonal wind difference (Last Millennium simulation) (m/s)	51
4.3	Composite sea level pressure difference (ERA-Interim reanalysis) (Pa) . .	52
4.4	Composite sea level pressure difference (Last Millennium simulation) (Pa)	52
4.5	IrrDJFM-CTR reference height temperature (K) (dotted: $p < 0.1$)	53
4.6	IrrDJFM-CTR total precipitation rate (mm/day) (dotted: $p < 0.1$)	53



4.7	IrrDJFM-CTR 200-hPa zonal wind (m/s) (dotted: $p < 0.1$)	54
4.8	IrrDJFM-CTR sea level pressure (Pa) (dotted: $p < 0.1$)	54
4.9	Differences (IrrDJFM-CTR) in reference height temperature over North America (K) (dotted: $p < 0.1$).	55
4.10	Differences (composite members-CTR) in SST globally (K).	55
4.11	Differences (composite members-CTR) in 500-hPa geopotential height (m).	56
4.12	Differences (composite members-CTR) in reference height temperature(K).	57
4.13	Differences (IrrAGCM-CtrAGCM) in reference height temperature over South Asia (K) (dotted: $p < 0.1$).	57
4.14	Differences (IrrAGCM-CtrAGCM) in 200-hPa velocity potential ($10^5 \text{ m}^2/\text{s}$) (dotted: $p < 0.1$)	58
4.15	Differences (IrrAGCM-CtrAGCM) in 500-hPa geopotential height (m) (dotted: $p < 0.1$).	59
4.16	Differences (IrrAGCM-CtrAGCM) in reference height temperature over North America (K) (dotted: $p < 0.1$).	60
5.1	PDO pattern. Taken from Deser et al. (2010)	60



List of Tables


2.1	Model setup	41
3.1	Simulated results averaged over IGP for different runs. Numbers in brackets are averaged over all India (0-40°N, 60-100°E)	41



Chapter 1


Introduction

Soil moisture is a critical component in the terrestrial hydroclimate and ecological system. The temporal and spatial distribution of soil moisture is pivotal for synoptic weather prediction and large scale climate simulation. Studies have shown that soil moisture can contribute to intraseasonal forecast skill (e.g., [Koster et al., 2010, 2011](#)). The importance of soil moisture lies in its control of both surface-energy balance and water balance ([Seneviratne et al., 2010](#)). Liquid soil water is transformed into water vapor in the process of evapotranspiration (ET) as the atmosphere absorbs latent heat from local land surfaces and can release the energy elsewhere. Depending on atmospheric circulation and conditions, the condensation of vapor results in cloud formation or in precipitation, which returns the water to the land surface. Coupled with air and precipitation, soil moisture can therefore interact with the climate.



Through various types of land use, humans are considerably influencing land surfaces. Among them, irrigation is the most direct act of changing soil moisture and thus should not be ignored. Adding water to a field to maintain soil moisture higher than unmanaged land causes evaporation from bare soil and transpiration from crops to increase. Previous studies have shown that irrigation has first-order effects on the near-surface climate through changes in local surface-energy partitioning (Douglas et al., 2006; Biggs et al., 2008) and generally leads to a lower Bowen ratio over the land, where the latent heat flux at the surface is increased and the sensible heat flux is decreased. Observations have also shown that air temperatures over heavily irrigated regions are lower because of evaporative cooling effects (Bonfils and Lobell, 2007; Roy et al., 2007; Lobell and Bonfils, 2008). Atmospheric model simulations have demonstrated that irrigation results in surface cooling and potentially enhances downwind precipitation (Yeh et al., 1984; Sacks et al., 2009; DeAngelis et al., 2010; Puma and Cook, 2010; Cook et al., 2011). In addition, modeling studies have revealed that irrigation affects atmospheric circulation in monsoonal regions including North America (Lo and Famiglietti, 2013; Lo et al., 2013), West Africa (Im et al., 2014), and South Asia (Saeed et al., 2009; Lee et al., 2011a; Guimberteau et al., 2012; Shukla et al., 2014), because these places are in climatic transition zones and are more sensitive to soil moisture deviations resulting from stronger land–atmosphere coupling strength (see Koster et al., 2006, for example).

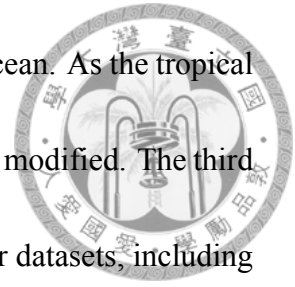
South Asia is the most heavily irrigated region of the world. Previous studies have



shown that the intensity, variability, and onset date of the summer monsoon are possibly affected by irrigation. Irrigation introduces additional moisture to the atmosphere; concurrently, evaporative cooling changes the thermal contrast between land and the ocean, thereby affecting moisture transport and the summer monsoon circulation. Studies so far focused on the impacts of irrigation during summertime mostly; however, high soil-moisture anomalies from irrigation might persist through fall and winter, and farmers still irrigate in low-latitude regions in the wintertime (discussed in more detail in Chapter 3.1), when the cool, dry air flows southward from the Indian subcontinent to the Indian Ocean as the prevailing South Asian winter monsoon. We investigated the extent to which the high soil-moisture anomalies of the wintertime affect the climate because of a substantial amount of irrigation water added to fields. The current study thus focuses on identifying the land–atmosphere interaction processes affected by water management and the consequent responses in atmospheric circulation over South Asia during the winter.

The purpose of this study is to investigate the following research issues. First, can we track the fingerprint of the irrigation here in observation data? If so, which means that the effects of irrigation are not negligible, then we would like to know the second question: Is the irrigation also affecting wintertime monsoon circulation and even have some remote impacts? We conduct state-of-the-art climate model simulations and analyze the results to answer the question. We will show that through change the intensity of South Asian winter monsoon, irrigation does have the potential to change not only local climate, but

also the precipitation patterns over Indian Ocean as well as Pacific Ocean. As the tropical circulation is perturbed, winter climate over North Pacific will also be modified. The third issue is to compare our findings with previous studies and some other datasets, including a last millennium simulation and reanalysis data. We use the two datasets to explore the impacts of South Asian winter monsoon on climate when there is no other interannual variation considered. The comparisons provide support on our hypothesized mechanisms of how irrigation in South Asia affects remote climate. The rest of this thesis is organized as follows. Chapter 2 briefly describes the data used and the setup of model experiments. Results are in Chapter 3. In Chapter 3.1 fingerprint of irrigation is detected from the observations we utilized. The rest of Chapter 3 are the results of a series of global climate model simulations. Chapter 4 discusses the results we found and provides some validation of the driving mechanism using different data sets. Finally, Chapter 5 is a summary of the results and the future work.





Chapter 2

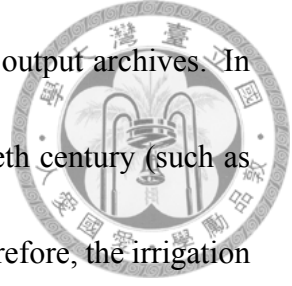
Methodology

2.1 Data sets

In this study, two sets of land-surface ET data were used for the analysis. One is a satellite-derived land ET record ([Zhang et al., 2010](#)) based on Advanced Very High Resolution Radiometer (AVHRR), and the other is an more in situ-based data set upscaled from the FLUXNET eddy-covariance towers using a machine-learning approach called model tree ensembles ([Jung et al., 2009](#)). Also used are the potential evapotranspiration (PET) data from the Climate Research Unit Time Series 3.2 data ([Harris et al., 2014](#)) and the data of irrigation water demand derived from agriculture and climate data sets ([Wisser et al., 2008](#)).

To isolate the effects of irrigation on the climate from other anthropogenic factors, we make use of the historical run of the NCAR Community Earth System Model (CESM)

from the Coupled Model Intercomparison Project Phase 5 (CMIP5) output archives. In this historical run, all the major anthropogenic forcing in the twentieth century (such as the aerosol) was included in the simulation but not the irrigation. Therefore, the irrigation effects on the climate are identified by comparing the historical run with the observations.

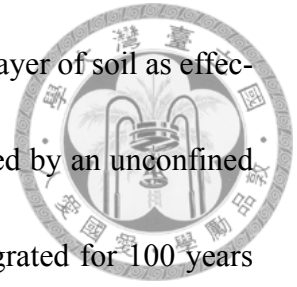


To elucidate the results we get in the model experiment, we also download the ERA-Interim reanalysis data and CMIP5 Community Climate System Model version 4 (CCSM4) last millennium simulations to analyze the effects of interannual variation of South Asian winter monsoon on climate.

2.2 Model setup

Numerical experiments were also conducted with the CESM to understand the mechanisms that enables irrigation to affect local and remote climates and the associated changes in atmospheric circulation. The experiments were performed with a fully coupled land–ocean–atmosphere configuration of the CESM, which includes the Community Atmosphere Model version 5 (CAM5) and the Community Land Model Version 4 (CLM4) that can explicitly simulate land hydrological processes (see Figure 2.1) and is suitable for the purpose of this study. A control (CTR) simulation and a perturbed (IRR) experiment were conducted, in which the global distribution and amount of irrigation estimated by [Wisser et al. \(2008\)](#) over the last decade of the twentieth century was included in the experiment

but not in the control simulation. The irrigation is applied to the top layer of soil as effective precipitation, with a quarter of the irrigation water being supplied by an unconfined aquifer (see Table 2.1 and Figure 2.2). Both simulations were integrated for 100 years with a horizontal model resolution of 1.9×2.5 degrees. The first 50 years were used as a model spin-up, whereas the last 50 years were used for analysis.





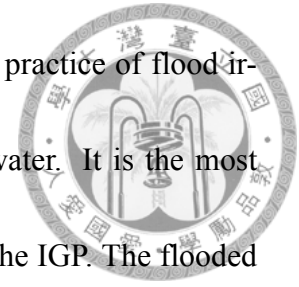
Chapter 3

Results

3.1 Regional impacts induced by the irrigation over the Indo-Gangetic Plain

Boreal winter is generally not the crop-growth season at northern midlatitudes because of low temperatures. The temperature is amenable at low latitudes to growing crops; however, it is the dry season, and irrigation is needed to compensate for the lack of moisture. Figure 3.1a shows a global estimate of irrigation water demand from agricultural and climate data sets (Wisser et al., 2008). Irrigation is concentrated in a few places (especially in South Asia) in boreal winter (January, February, and March; JFM). The belt of irrigation clearly observed over Northern India is the Indo-Gangetic Plain (IGP), which can be seen having the irrigation amount about an order of magnitude larger than elsewhere.

A substantially large amount of water used there is attributed to the practice of flood irrigation, which floods the field to facilitate soaking the soil with water. It is the most water consuming method of irrigation and is commonly adopted in the IGP. The flooded fields behave like ponds and continuously evaporate moisture into the lowest level of the atmosphere.

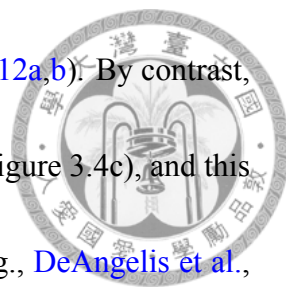


In regions where the PET is higher than the actual ET, previous studies have indicated that there is possibly a direct effect of increased latent heat fluxes to the atmosphere in response to excess soil moisture (e.g., [Seneviratne et al., 2010](#)). In addition, in this region, a considerable portion of the irrigation water is withdrawn from groundwater. Such a large amount of groundwater withdrawal has been observed over Northern India by NASA Gravity Recovery and Climate Experiment (GRACE) satellites ([Rodell et al., 2009](#)). As groundwater (particularly confined groundwater) is originally inactive in the water cycle, the withdrawal is thus in effect adding additional water to participate in land–atmosphere interactions (Figure 3.2).

Irrigation constitutes a critical part of moisture supply to the ET; Figure 3.1b shows a comparison of the mean seasonal cycles of PET, observed ET, and irrigation amount in the IGP. The AVHRR-based, FLUXNET-based and PET data from CRU are averaged over 1983-2006, 1982-2011 and 1981-2000, respectively. While the PET curve is unimodal and peaked in the early summer, both the irrigation amount and actual ET curves are bimodal and peaked in spring and early fall. The similarity between the irrigation amount and

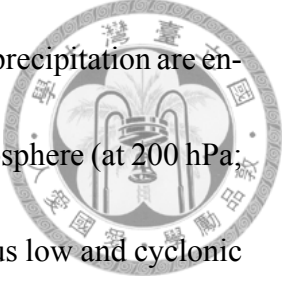
the ET illustrates the crucial role that irrigation plays in the ET. Furthermore, without considering the effect of irrigation, the ET simulated by the historical run of the CESM in JFM is underestimated compared with that estimated by both remote-sensing and in-situ observations (Figure 3.1c). In addition, compared with the whole Indian subcontinent, near-surface temperature simulated by CESM over IGP has a relative warm bias when compared with CRU grid data (Figure 3.3). Therefore, the large amount of irrigation water applied in the IGP has most likely left a fingerprint in local water and energy balance that can act as a potential forcing to regional or even remote climate. It is necessary to understand what and how the irrigation over South Asia practices impact the climate.

To identify the local climate response to the irrigation over South Asia, we compared and show in Figure 3.4 and Table 3.1 the simulation differences between the CTR and IRR simulations in JFM. Over the South Asia, the irrigation increases the soil water in the top 10 cm of the soil layer (Figure 3.4a) and the latent heat fluxes into the atmosphere (Figure 3.4b). The mean latent heat release in the IGP changed from 25.92 W/m² in the CTR simulation to 37.74 W/m² in the IRR simulation. The latter value is reasonably close to the value of the observed latent heat flux shown in Figure 3.4c. We note that the largest increases of soil water and latent heat fluxes occur in the heavily irrigated regions (cf. Figure 3.4a and 3.4b to Figure 3.1a). Since the South Asia is located in the subsidence branch of the Hadley circulation during the boreal winter, the increased input of the moisture to the atmosphere by the irrigation does not induce more precipitation locally,



which has been implied by previous studies ([Harding and Snyder, 2012a,b](#)). By contrast, low-level cloud cover increases downwind of the irrigated regions (Figure 3.4c), and this finding is consistent with the irrigation studies in North America (e.g., [DeAngelis et al., 2010](#); [Lo and Famiglietti, 2013](#)). The increased cloudiness decreases the downward solar radiation at the surface (Figure 3.4d) to cause a surface cooling that spreads throughout the entire Indian subcontinent (Figure 3.4e). The results imply that the local responses to irrigation are not always the same and dependent on the background climate and season it is applied. The surface air temperature in the IGP region decreases by about 1°C from the CTR simulation to the IRR simulation. It is necessary to point out that surface temperature in IGP was projected to increase 4.5°C by the end of twenty-first century without considering the irrigation effect in the 8.5 W/m² representative concentration pathways (RCP8.5) simulation of CESM. The project can thus be different if the irrigation impacts are included.

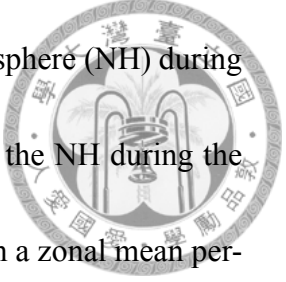
The intensity of the Indian monsoon circulation is associated with the land–sea thermal contrast between the Indian subcontinent and the Indian Ocean. Therefore, the cooling induced by the irrigation over the Indian subcontinent can result in a larger sea-land contrast to enhance the winter Indian monsoon. This is confirmed by simulation difference produced by the CTR and IRR simulations in Figure 3.5a, which shows the low-level (925 hPa) northeast winds intensified over northeast South Asian and the western Arabian Sea. The anomalous northeasterlies move across the equator into an anomalous low over the



tropical western Indian Ocean, where the upward vertical velocity and precipitation are enhanced. The monsoonal flow then returns northward in the upper troposphere (at 200 hPa; Figure 3.5b) and subsides over the India Peninsula where an anomalous low and cyclonic circulation were produced. The anomalous meridional circulation associated with this enhanced winter monsoon circulation is shown in Figure 3.5c, where the zonally-averaged (40°E-90°E) omega velocity is shown. The figure shown that descending motion is enhanced over the northern Indian (around 30°N) while the ascending is enhanced over the Southern Indian Ocean (around 30°S). The 200-hPa velocity potential anomalies shown in Figure 3.5e clearly indicate an anomalous convergence over South Asia and an anomalous divergence over the tropical Indian Ocean. These features together indicate that the IGP irrigation can induce an intensified winter monsoonal circulation and local Hadley cell, which are illustrated in Figure 3.5d.

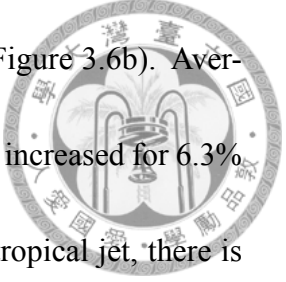
3.2 Remote impacts on the North American winter climate

The strength of the Hadley circulation is known to be sensitive to the latitudinal displacement of the solar heating ([Lindzen and Hou, 1988](#)), which makes the Hadley circulation to be most prominent during boreal winter when the strongest solar displaces to the south of the equator. The Hadley cell transports energy in the direction of its up-



per branch from the Southern Hemisphere (SH) to the Northern Hemisphere (NH) during the winter. The irrigation-induced surface cooling is concentrated in the NH during the winter, thus increasing the interhemispheric temperature gradient from a zonal mean perspective. The interhemispheric temperature gradient is crucial for tropical rainfall and the Hadley circulation, and the concept has been employed in studies on paleoclimatic scenarios, present day climatic variations, and anthropogenic aerosol forcings to assess the effects of interhemispheric-asymmetric thermal forcing (e.g., [Chiang and Bitz, 2005](#); [Broccoli et al., 2006](#); [Bollasina et al., 2011](#); [Lee et al., 2011b](#); [Chiang and Friedman, 2012](#); [Swann et al., 2012](#); [Friedman et al., 2013](#); [Hwang et al., 2013](#)). A higher interhemispheric temperature gradient tends to transport more energy between the hemispheres.

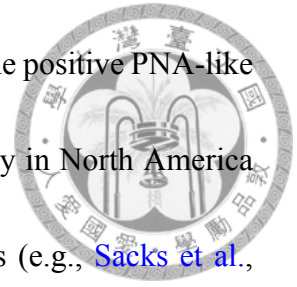
The changes in the zonal mean stream function between the CTR and IRR simulations (Figure 3.6a) show an intensification of Hadley circulation in response to the boreal cooling induced by irrigation, which is in accordance with the local Hadley cell change over Indian Ocean sector. As the Hadley circulation is intensified in a global manner, the tropical precipitation changes are found in not only Indian Ocean but also other basins, notably Pacific Ocean. In general, precipitation north to Australia is suppressed, and the tropical rain belt over central Pacific Ocean is shifted southward (Figure 3.7). Taking the zonal mean of precipitation change, it is seen more clearly that tropical precipitation is displaced southward (Figure 3.8). The changes in the tropical circulation cause more angular momentum to be transported to the NH midlatitudes and result in an intensification



of the subtropical jet, centered over the northeastern Pacific Ocean (Figure 3.6b). Averaged from 150°E to 120°W, the 200-hPa zonal wind speed at 30°N has increased for 6.3% (from 50.9 m/s to 54.1 m/s). Following the strengthening of the subtropical jet, there is anomalous westward wind velocity north to 45°N. The weakening of mid-latitude westerlies is a manifestation of weakened transient eddy activity over North Pacific, which has been shown in observational and theoretical studies associated with a strengthened subtropical jet (Nakamura, 1992, 2002; Lee and Kim, 2003). The resulting anomalous cyclonic circulation exhibits a barotropic structure and corresponds with a deepening and eastward shift of the semipermanent Aleutian low, as observed from sea-level pressure differences (Figure 3.6c). The prevailing winter weather pattern or storm track is related to the position and strength of the jet stream. These changes in the northeastern Pacific resemble the positive Pacific/North American (PNA) pattern, and are indications of North Pacific winter climatic change, the remote impacts of wintertime irrigation over Asian low latitudes (e.g. Trenberth et al., 1998).

Figure 3.9b shows the differences in surface air temperature over North America between the CTR and IRR simulations, which interestingly exhibit anomalous warming in west to central North America despite the lack of irrigation in North America during the winter season. These differences are thus another manifestation of the remote impacts of irrigation at Asian low latitudes, which is in accordance with the circulation changes revealed in Figure 3.6 over the northeastern Pacific. The deepened Aleutian low and ridg-

ing across western North America (see Figure 3.9a) associated with the positive PNA-like pattern results in above-normal temperatures. The warming tendency in North America has also been seen in several previous studies on irrigation impacts (e.g., [Sacks et al., 2009](#); [Puma and Cook, 2010](#); [Cook et al., 2014](#)), which utilized either models or irrigation schemes that are different from the current study. As previous studies did not explicitly explain the origin of the warming tendency in North America, the current study provides a plausible mechanism, which is induced by the irrigation activity in Asian low-latitudes.





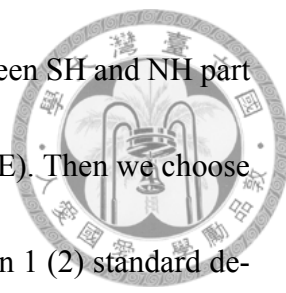
Chapter 4

Discussion

In this chapter, we provide some examinations on the results we find in the simulations. First we focus on the impacts of South Asian winter monsoon variability from Indian subcontinent surface temperature on northeastern Pacific. Then we compare the current study with some previous studies to show that our findings are not odd exceptions. We note that the current study implies not only the potential of land processes at Indian subcontinent affecting winter monsoon but also the sensitivity of tropical and northeastern Pacific atmosphere to Indian Ocean SST and precipitation anomalies.

4.1 Remote impacts of winter monsoon variability

There are about 30 and 1000 years of data in ERA-Interim reanalysis and CCSM4 last millennium simulations, respectively. We define an Indian interhemispheric temperature

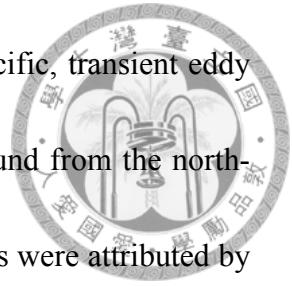


gradient, $\Delta T = T_{SH} - T_{NH}$, which is the temperature difference between SH and NH part of Indian basin (T_{SH} is 0-30°S, 40-100°E and T_{NH} is 0-30°N, 40-100°E). Then we choose the winters with largest and smallest ΔT (ΔT larger and smaller than 1 (2) standard deviations for ERA-Interim (last millennium simulations)) and take their differences of sea level pressure and upper level zonal wind velocity (Figures 4.1, 4.2, 4.3, 4.4). It is known that ENSO has prominent influences on extratropical circulation (e.g. [Horel and Wallace, 1981](#); [Wallace and Gutzler, 1981](#)). But meanwhile, it also influences the Indian Ocean simultaneously. To remove the influences of ENSO, we should only composite years with neutral phase of ENSO. Therefore, we only choose years with absolute values of normalized Niño3.4 index smaller than 1(0.1) for ERA-Interim (last millennium simulations) in our composites. In Figures 4.1, 4.2, 4.3, 4.4, it can be seen that in both the reanalysis and last millennium simulations, Aleutian Low is deepened and the subtropical jet over northeastern Pacific is intensified when ΔT is larger. The results clearly illustrate the potential linkage of Indian subcontinent surface temperature and thus South Asian winter monsoon and northeastern Pacific climate.

The potential influences of monsoons to remote climates have been studied using Paleoclimate Model Intercomparison Project Phase 2 (PMIP2) models, in which [Chiang and Fang \(2010\)](#) found notable differences in wintertime northeastern Pacific sea-level pressure and Pacific jet-stream intensity in mid-Holocene simulations. Compared with present-day simulations, [Chiang and Fang \(2010\)](#) found that the Aleutian low was deep-

ened, the subtropical jet stream intensified near the northeastern Pacific, transient eddy activity reduced in the main storm-track region, and colder SST found from the northwestern to central Pacific. The differences in the mean climatic states were attributed by the authors to a stronger seasonality, which is due to different insolation caused by precessional forcing. In association with a stronger seasonality, the monsoon intensity in the mid-Holocene was stronger than in the present day and the tropical rainfall was also changed. The results thus shared the same mechanism as that in the current study.

In the current study, we provide an example of how a comprehensive earth system model responds to an interhemispheric thermal asymmetry in the boreal winter season. The results from such a model can be compared to those from models of intermediate complexity because the adjustment to the forcing in the current study was accomplished through South Asian winter monsoon circulation. The zonal connection of the tropical Indian Ocean and Pacific Ocean is essential in inducing climatic modifications over the northeastern Pacific and North America. The dynamical mechanisms of this connection warrant further research. The results also imply a climatic hotspot in the South Asian regions. Because it involves an immense land mass facing the Indian Ocean and located at rather low latitude, modifications of land-surface conditions in South Asia can have the potential to affect remote regions.



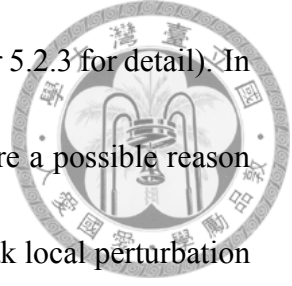
4.2 Memory effects of soil moisture anomalies



It is known that soil moisture anomalies possess the memory effect, through propagating the anomalies into deeper soil layer or land subsurface. The high soil moisture anomalies we observed in the experiment thus come from not only wintertime irrigation but also the enormous amount of irrigation applied in the post-monsoon season. To separate the effects of irrigation in wintertime and prior-to-winter season, we also conduct an additional experiment in which we only apply irrigation at low latitudes (0-40°N) in the wintertime (DJFM). It turned out that in the winter-irrigation-only simulation (hereafter IrrDJFM), the cooling over Indian subcontinent is not that spread (cf. Figures 4.5 and 3.4e). However, there is still eastward shift of tropical rainfall in tropical Indian Ocean and drying north to Australia presented (cf. Figures 4.6 and 3.7). And we can still see most of the remote impacts presented in the IRR-CTR comparison, but with smaller amplitudes. These include deepened Aleutian low, intensified subtropical jet over northeastern Pacific and warming western North America (Figures 4.7, 4.8, 4.9).

How does the influence of the smaller perturbation make its way to the northeastern Pacific? Some literature have shown that northeastern Pacific is susceptible to forcing from certain regions. In works of [Simmons et al. \(1983\)](#), they found forcing from Southeast Asia being an effective source exciting the PNA-like pattern and in [Molteni et al. \(2015\)](#), positive precipitation anomalies over tropical western Indian Ocean were shown

to have contribution to the positive PNA-like pattern, too (see Chapter 5.2.3 for detail). In the current study, the two are both presented as forcing; it is therefore a possible reason why the teleconnection pattern is sensitive despite the seemingly weak local perturbation over South Asia and it thus lend us confidence that the results in current study are consistent with previous studies in terms of the cross basin impacts of Indian Ocean to the Pacific.

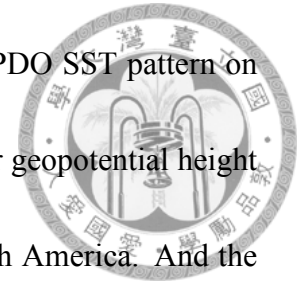


4.3 Teleconnection without tropical influences

As both upper level convergence over Southeast Asia and tropical influence are constructive for positive PNA-like pattern, it is interesting to clarify their respective contributions. We would like to know whether the remote response still exists if only South Asian local forcing (i.e., upper level convergence) is considered. Two ways of analyses are utilized to rule out the influence from long-term SST fluctuations.

First, we subjectively choose years from IRR with their SST over 30° - 45° N, 150° E- 150° W, where the Pacific Decadal Oscillation (PDO) pattern is prominent (see Chapter 5.2.3), being as close as possible to that of CTR simulation to have composite analysis. The 66th, 67th, 76th, 81th, 96th and 100th years are the chosen members. The mean SST of the selected members over the selected region is 285.879 K, and in CTR it is 285.877 K. The composite SST difference is shown in Figure 4.10, and the SST dipole pattern over

mid-latitude in Pacific Ocean is largely eliminated. The effects of PDO SST pattern on atmosphere are thus eliminated. Figure 4.11 shows at 500 hPa lower geopotential height in the vicinity of Aleutian islands and ridging over continental North America. And the warming tendency over North America is prominent (Figure 4.12).



On the other hand, we also conduct additional experiments in AGCM (i.e., the SST in the simulations is fixed) with all other model setup being the same as in CTR and IRR. This set of simulation, denoted IrrAGCM and CtrAGCM hereafter, still possesses the teleconnection pattern. There is still spread cooling over Indian subcontinent (Figure 4.13). The upper level convergence over South Asia is located more westward compared with Figure 3.5e and Figure 5 in [Simmons et al. \(1983\)](#) (Figure 4.14); however, as the model complexities as well as configurations in [Simmons et al. \(1983\)](#) and the current work are quite different, it is still qualitatively possible that the upper level convergence associated with local surface cooling is able to induce PNA teleconnection pattern. As for the remote impact, inspecting from 500-hPa geopotential height, the positive PNA pattern is still clear, and the warming anomalies over North America are significant (Figures 4.15 and 4.16). In these experiments, the SSTs are fixed so that the tropical influences via SST are not possible to affect extratropical circulation. Through this series of analysis and experiments, we demonstrate that even without long-term SST fluctuations, the forcing from South Asian irrigation can still induce the PNA teleconnection pattern with a smaller amplitude.

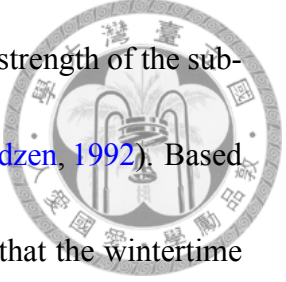


Chapter 5

Conclusion

5.1 Summary

In this study, we addressed the critical effect of agricultural irrigation in Asian low latitudes on the winter climate. The control simulation, which did not consider irrigation, underestimates the latent heat flux over the intensively irrigated region of the IGP; by contrast, increased low cloud cover in the IRR simulation spread the original evaporative cooling (from excess ET) to the Indian subcontinent scale. The cooling over the Indian subcontinent makes a larger land–sea thermal contrast between the tropical Indian Ocean and the Indian subcontinent. The low-level northeasterly wind strengthens approximately 5% over the Indian subcontinent and west Arabian Sea. The Hadley circulation transports angular momentum from the tropical region to the subtropical region, thus affecting the intensity of the subtropical jet. Previous theoretical studies have shown that the meridional

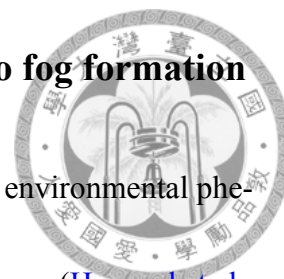


shift of the tropical rain belt influences the Hadley circulation and the strength of the subtropical jet (Held and Hou, 1980; Lindzen and Hou, 1988; Hou and Lindzen, 1992). Based on state-of-the-art earth-system-model simulations, this study shows that the wintertime wet soil-moisture anomalies induced by irrigation at low latitudes is likely to enhance the zonal mean atmospheric circulation in a cross-basin manner and affect wintertime storm tracking in the northeastern Pacific because of the hemispheric asymmetric distribution of the irrigation applied. The tropical–extratropical climatic interaction is established with the intensified, zonal mean Hadley circulation. The upper-level jet stream system is modified in the NH, and the Aleutian low is deepened and shifts eastward. The anthropogenic perturbation of climates is highly dynamic with time evolution, geographical distribution, and even cultural backgrounds. Therefore, to generate a climate simulation that is more realistic (particularly for future climate projections), it is crucial to understand in detail the South Asian land use and management such as the irrigation discussed in this study.

5.2 Future works

This study raises several questions that worth further query, including meteorological and climatic issues; they are also among different spatial and time scales. The followings are some examples.

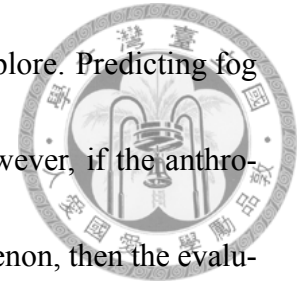
5.2.1 Influences of moisture supply from irrigation to fog formation



The winter fog in northeastern Pakistan and India is an important environmental phenomenon. The fog causes extensive economic and public health damages (Hameed et al., 2000). During foggy days, the visibility decreased from larger than 10000 meters to smaller than 200 meters (Yasmeen et al., 2012). Fog frequency has been increased in the past few decades, and it has been associated with the large amount of aerosol emission from biomass burning in surrounding regions (Gautam et al., 2007; Gautam, 2014). High aerosol loads are important for formation of fog events and can enhance the fog duration and intensity but only under certain meteorological condition. Some specific meteorological conditions favourable for fog formation have been identified, and temperature, relative humidity, wind speed and elevation are found relevant to fog formation (Saraf et al., 2011). The aerosol impacts have already received some attention, but it is also needed to know if the change of moisture content interacts with the already-known increases of aerosol loading. As the irrigation can largely modify the near-surface air humidity, it thus also influences the phenomenon and needed to be studied.


Following the methodology of previous studies, satellite data and local meteorological observation should be used to study some of the major events. Information of irrigation applied near the fog events will also be needed to clarify their relation. Also, how does irrigation pattern change during the past few decades, and in what extent has it changed

the near-surface condition? These questions are also important to explore. Predicting fog events is not simple given the limitation of operational model. However, if the anthropogenic water management in reality also contributes to the phenomenon, then the evaluation would be useful for operation fog prediction. Finally, given all the factors relevant to fog is considered, its long-term trend can thus also be studied.



5.2.2 Irrigation in West Asia impacts to glacier status in Tibetan Plateau and surroundings

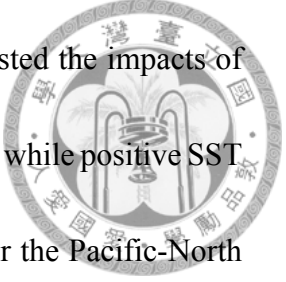
The glaciers in Tibetan Plateau and its surrounding regions are important as they are at the headwaters of many rivers. It is found that the glacier status is associated with atmospheric circulation patterns and in different regions the glaciers are having different trends. In the Himalayas, glaciers are generally experiencing retreat but in eastern Pamir it is reported the glacier might have been advancing recently (Yao et al., 2012). The differences came from the different types of precipitation the glaciers in different regions received. In Yao et al. (2012), they attributed the increase of precipitation in eastern Pamir to the intensification of westerlies in wintertime, and retreat of Himalaya glaciers to the weakening of summer monsoon. However, much irrigation is also applied in West Asia as groundwater depletion can already be observed from satellite (see Voss et al., 2013, for example), and west Asia is on the track of the westerlies bringing moisture to the eastern Pamir region.



On the other hand, in addition to eastern Pamir region, western Himalayas also receive precipitation in winter. The Western Disturbances (WDs) are also related to westerly jet stream and they move eastward from Mediterranean Sea bringing moisture to Pakistan and Northern India. Previous study has noticed the possibilities of irrigation to modify high level atmospheric circulation and weaken the jet strength (Lee et al., 2011a). Does the human activities on the pathways of WDs affect moisture supply and even jet strength? In addition, does the irrigation at West Asia leave its fingerprint on local hydroclimate as we found in the South Asia? These are also important questions to answer.

5.2.3 Cross basin influences of Indian Ocean

In addition to the mid-Holocene experiment, there are also studies focusing on cross basin influences of tropical Indian Ocean during boreal winter. For example, SST and precipitation anomalies in the tropical Indian Ocean exhibit prominent interdecadal fluctuations and are found to play a role in the interdecadal climate variability over the North Pacific during boreal winter (Cole, 2000; Deser et al., 2004). It is also found that having more realistic precipitation in model over tropical Indian Ocean is important for simulating the phase change of Pacific Decadal Oscillation (PDO) in 1970s (Deser and Phillips, 2006). PDO, defined as the leading EOF of monthly SST anomalies over the North Pacific (Mantua et al., 1997), is a coupled ocean-atmosphere climate variability of decadal time scale (Figure 5.1) and the Aleutian low is observed to fluctuate with its variations



(Deser et al., 2004). Using AGCM as tools, previous studies have tested the impacts of Indian Ocean SST anomalies on NH circulation. It was pointed out that while positive SST anomalies over Pacific Ocean during El Niño have the effect of lower the Pacific-North American (PNA) region geopotential height, i.e., deepen the Aleutian low, the contribution from tropical Indian Ocean has the opposite sign to that of Pacific Ocean (Barsugli and Sardeshmukh, 2002; Annamalai et al., 2005, 2007). However, recently in Molteni et al. (2015), they found that as in west Pacific and most of Indian Ocean the SST does not correlate well with precipitation anomalies, the teleconnection relation should be evaluated using precipitation instead of SST anomalies. They separated the Indian Ocean into the western and central Indian Ocean (WCIO) and the eastern Indian Ocean to the western edge of the Pacific (EIWP) and found that the teleconnections between Indo-Pacific precipitation anomalies and North Pacific 500-hPa geopotential height is a tri-polar structure with two positively correlated centers in WCIO and central Pacific, and the third one in EIWP, being anti-correlated with the other two.

In the current study, the results match the conclusions of Molteni et al. (2015) that we found positive PNA-like pattern with negative precipitation anomalies north to Australia and positive anomalies over tropical western Indian Ocean. However, what is the dynamical mechanism of this cross basin connection? Previous studies used exclusively most AGCM to study this issue, but Indian Ocean is subject to seasonal transition of wind direction and having monsoonal ocean current following the direction of monsoon flow.

Is the feedback of Indian Ocean to the atmosphere playing a role in the zonal climatic connection? Is it via the ocean or the atmosphere? The answers to these questions are of great importance and have their implication not only in the intraseasonal but also interdecadal time scale, as the PDO is thought to some extent being forced from tropical ocean. Using comprehensive coupled models, we will be able to investigate the problem more clearly and more directly.





Bibliography

Annamalai, H., P. Liu, and S. P. Xie, 2005: Southwest Indian Ocean SST variability:

Its local effect and remote influence on Asian monsoons. *Journal of Climate*, **18 (20)**, 4150–4167, doi:10.1175/JCLI3533.1.

Annamalai, H., H. Okajima, and M. Watanabe, 2007: Possible impact of the Indian

Ocean SST on the Northern Hemisphere circulation during El Niño. *Journal of Climate*, **20 (13)**, 3164–3189, doi:10.1175/JCLI4156.1.

Barsugli, J. J., and P. D. Sardeshmukh, 2002: Global atmospheric sensitivity to tropical

SST anomalies throughout the Indo-Pacific basin. *Journal of Climate*, **15 (23)**, 3427–3442, doi:10.1175/1520-0442(2002)015<3427:GASTTS>2.0.CO;2.

Biggs, T. W., C. a. Scott, A. Gaur, J. P. Venot, T. Chase, and E. Lee, 2008: Impacts of

irrigation and anthropogenic aerosols on the water balance, heat fluxes, and surface temperature in a river basin. *Water Resources Research*, **44 (12)**, 1–18, doi:10.1029/2008WR006847.

Bollasina, M. a., Y. Ming, and V. Ramaswamy, 2011: Anthropogenic Aerosols and the Weakening of the South Asian Summer Monsoon. *Science*, **334 (6055)**, 502–505, doi:10.1126/science.1204994.



Bonfils, C., and D. Lobell, 2007: Empirical evidence for a recent slowdown in irrigation-induced cooling. *Proceedings of the National Academy of Sciences of the United States of America*, **104 (34)**, 13 582–13 587, doi:10.1073/pnas.0700144104.

Broccoli, A. J., K. a. Dahl, and R. J. Stouffer, 2006: Response of the ITCZ to Northern Hemisphere cooling. *Geophysical Research Letters*, **33 (1)**, 1–4, doi:10.1029/2005GL024546.

Chiang, J. C., and A. R. Friedman, 2012: Extratropical Cooling, Interhemispheric Thermal Gradients, and Tropical Climate Change. *Annual Review of Earth and Planetary Sciences*, **40 (1)**, 383–412, doi:10.1146/annurev-earth-042711-105545.

Chiang, J. C. H., and C. M. Bitz, 2005: Influence of high latitude ice cover on the marine Intertropical Convergence Zone. *Climate Dynamics*, **25 (5)**, 477–496, doi:10.1007/s00382-005-0040-5.

Chiang, J. C. H., and Y. Fang, 2010: Was the north Pacific wintertime climate less stormy during the mid-Holocene? *Journal of Climate*, **23 (14)**, 4025–4037, doi:10.1175/2010JCLI3510.1.

Cole, J. E., 2000: Tropical Pacific Forcing of Decadal SST Variability in the Western Indian Ocean over the Past Two Centuries. *Science*, **287** (5453), 617–619, doi:10.1126/science.287.5453.617.



Cook, B. I., M. J. Puma, and N. Y. Krakauer, 2011: Irrigation induced surface cooling in the context of modern and increased greenhouse gas forcing. *Climate Dynamics*, **37** (7-8), 1587–1600, doi:10.1007/s00382-010-0932-x.

Cook, B. I., S. P. Shukla, M. J. Puma, and L. S. Nazarenko, 2014: Irrigation as an historical climate forcing. *Climate Dynamics*, doi:10.1007/s00382-014-2204-7.

DeAngelis, A., F. Dominguez, Y. Fan, A. Robock, M. D. Kustu, and D. Robinson, 2010: Evidence of enhanced precipitation due to irrigation over the Great Plains of the United States. *Journal of Geophysical Research: Atmospheres*, **115** (15), 1–14, doi:10.1029/2010JD013892.

Deser, C., M. a. Alexander, S.-P. Xie, and A. S. Phillips, 2010: Sea surface temperature variability: patterns and mechanisms. *Annual review of marine science*, **2**, 115–143, doi:10.1146/annurev-marine-120408-151453.

Deser, C., and A. S. Phillips, 2006: Simulation of the 1976/77 climate transition over the North Pacific: Sensitivity to tropical forcing. *Journal of Climate*, **19** (23), 6170–6180, doi:10.1175/JCLI3963.1.

Deser, C., A. S. Phillips, and J. W. Hurrell, 2004: Pacific interdecadal climate variability: Linkages between the tropics and the North Pacific during boreal winter since 1900. *Journal of Climate*, **17** (16), 3109–3124, doi:10.1175/1520-0442(2004)017<3109: PICVLB>2.0.CO;2.



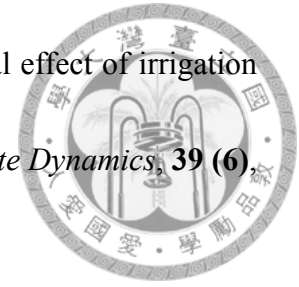
Douglas, E. M., D. Niyogi, S. Frohking, J. B. Yeluripati, R. a. Pielke, N. Niyogi, C. J. Vörösmarty, and U. C. Mohanty, 2006: Changes in moisture and energy fluxes due to agricultural land use and irrigation in the Indian Monsoon Belt. *Geophysical Research Letters*, **33** (14), 1–5, doi:10.1029/2006GL026550.

Friedman, A. R., Y. T. Hwang, J. C. H. Chiang, and D. M. W. Frierson, 2013: Interhemispheric temperature asymmetry over the twentieth century and in future projections. *Journal of Climate*, **26** (15), 5419–5433, doi:10.1175/JCLI-D-12-00525.1.

Gautam, R., 2014: Challenges in Early Warning of the Persistent and Widespread Winter Fog over the Indo-Gangetic Plains: A Satellite Perspective. *Reducing Disaster: Early Warning Systems For Climate Change SE - 3*, A. Singh, and Z. Zommers, Eds., Springer Netherlands, 51–61, doi:10.1007/978-94-017-8598-3_3.

Gautam, R., N. C. Hsu, M. Kafatos, and S. C. Tsay, 2007: Influences of winter haze on fog/low cloud over the Indo-Gangetic plains. *Journal of Geophysical Research: Atmospheres*, **112** (5), 1–11, doi:10.1029/2005JD007036.

Guimberteau, M., K. Laval, A. Perrier, and J. Polcher, 2012: Global effect of irrigation and its impact on the onset of the Indian summer monsoon. *Climate Dynamics*, **39** (6), 1329–1348, doi:10.1007/s00382-011-1252-5.



Hameed, S., and Coauthors, 2000: On the widespread winter fog in Northeastern Pakistan and India. *Geophysical Research Letters*, **27** (13), 1891–1894, doi:10.1029/1999GL011020.

Harding, K. J., and P. K. Snyder, 2012a: Modeling the Atmospheric Response to Irrigation in the Great Plains. Part I: General Impacts on Precipitation and the Energy Budget. *Journal of Hydrometeorology*, **13** (6), 1667–1686, doi:10.1175/JHM-D-11-098.1.

Harding, K. J., and P. K. Snyder, 2012b: Modeling the Atmospheric Response to Irrigation in the Great Plains. Part II: The Precipitation of Irrigated Water and Changes in Precipitation Recycling. *Journal of Hydrometeorology*, **13** (6), 1687–1703, doi:10.1175/JHM-D-11-099.1.

Harris, I., P. D. Jones, T. J. Osborn, and D. H. Lister, 2014: Updated high-resolution grids of monthly climatic observations - the CRU TS3.10 Dataset. *International Journal of Climatology*, **34** (3), 623–642, doi:10.1002/joc.3711.

Held, I. M., and A. Y. Hou, 1980: Nonlinear Axially Symmetric Circulations in a Nearly



Inviscid Atmosphere. *Journal of the Atmospheric Sciences*, **37 (3)**, 515–533, doi:10.1175/1520-0469(1980)037<0515:NASCIA>2.0.CO;2.

Horel, J. D., and J. M. Wallace, 1981: Planetary-scale phenomena associated with the Southern Oscillation. *Mon. Wea. Rev.*, **109 (10)**, 813–829, doi:10.1175/1520-0493(1981)109<0813:PSAPAW>2.0.CO;2.

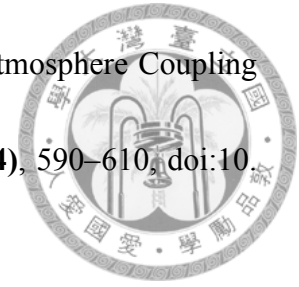
Hou, A. Y., and R. S. Lindzen, 1992: The Influence of Concentrated Heating on the Hadley Circulation. *Journal of the Atmospheric Sciences*, **49 (14)**, 1233–1241, doi:10.1175/1520-0469(1992)049<1233:TIOCHO>2.0.CO;2.

Hwang, Y. T., D. M. W. Frierson, and S. M. Kang, 2013: Anthropogenic sulfate aerosol and the southward shift of tropical precipitation in the late 20th century. *Geophysical Research Letters*, **40 (11)**, 2845–2850, doi:10.1002/grl.50502.

Im, E. S., M. P. Marcella, and E. a. B. Eltahir, 2014: Impact of potential large-scale irrigation on the West African monsoon and its dependence on location of irrigated area. *Journal of Climate*, **27 (3)**, 994–1009, doi:10.1175/JCLI-D-13-00290.1.

Jung, M., M. Reichstein, and A. Bondeau, 2009: Towards global empirical upscaling of FLUXNET eddy covariance observations: validation of a model tree ensemble approach using a biosphere model. *Biogeosciences Discussions*, **6 (3)**, 5271–5304, doi:10.5194/bgd-6-5271-2009.

Koster, R. D., and Coauthors, 2006: GLACE: The Global Land–Atmosphere Coupling Experiment. Part I: Overview. *Journal of Hydrometeorology*, **7** (4), 590–610, doi:10.1175/JHM510.1.



Koster, R. D., and Coauthors, 2010: Contribution of land surface initialization to subseasonal forecast skill: First results from a multi-model experiment. *Geophysical Research Letters*, **37** (2), 1–6, doi:10.1029/2009GL041677.

Koster, R. D., and Coauthors, 2011: The Second Phase of the Global Land–Atmosphere Coupling Experiment: Soil Moisture Contributions to Subseasonal Forecast Skill. *Journal of Hydrometeorology*, **12** (5), 805–822, doi:10.1175/2011JHM1365.1.

Lee, E., W. J. Sacks, T. N. Chase, and J. a. Foley, 2011a: Simulated impacts of irrigation on the atmospheric circulation over Asia. *Journal of Geophysical Research: Atmospheres*, **116** (8), 1–13, doi:10.1029/2010JD014740.

Lee, S., and H.-k. Kim, 2003: The Dynamical Relationship between Subtropical and Eddy-Driven Jets. *Journal of the Atmospheric Sciences*, **60** (12), 1490–1503, doi:10.1175/1520-0469(2003)060<1490:TDRBSA>2.0.CO;2.

Lee, S. Y., J. C. H. Chiang, K. Matsumoto, and K. S. Tokos, 2011b: Southern Ocean wind response to North Atlantic cooling and the rise in atmospheric CO₂: Modeling



perspective and paleoceanographic implications. *Paleoceanography*, **26** (1), 1–16, doi:10.1029/2010PA002004.

Lindzen, R. S., and A. V. Hou, 1988: Hadley Circulations for Zonally Averaged Heating Centered off the Equator. *Journal of the Atmospheric Sciences*, **45** (17), 2416–2427, doi:10.1175/1520-0469(1988)045<2416:HCFZAH>2.0.CO;2.

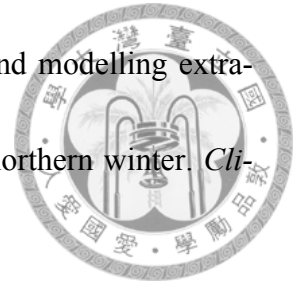
Lo, M. H., and J. S. Famiglietti, 2013: Irrigation in California's Central Valley strengthens the southwestern U.S. water cycle. *Geophysical Research Letters*, **40** (2), 301–306, doi:10.1002/grl.50108.

Lo, M. H., C. M. Wu, H. Y. Ma, and J. S. Famiglietti, 2013: The response of coastal stratocumulus clouds to agricultural irrigation in California. *Journal of Geophysical Research: Atmospheres*, **118** (12), 6044–6051, doi:10.1002/jgrd.50516.

Lobell, D. B., and C. Bonfils, 2008: The effect of irrigation on regional temperatures: A spatial and temporal analysis of trends in California, 1934–2002. *Journal of Climate*, **21** (10), 2063–2071, doi:10.1175/2007JCLI1755.1.

Mantua, N. J., S. R. Hare, Y. Zhang, J. M. Wallace, and R. C. Francis, 1997: A Pacific Interdecadal Climate Oscillation with Impacts on Salmon Production. *Bulletin of the American Meteorological Society*, **78** (6), 1069–1079, doi:10.1175/1520-0477(1997)078<1069:APICOW>2.0.CO;2.

Molteni, F., T. N. Stockdale, and F. Vitart, 2015: Understanding and modelling extra-tropical teleconnections with the Indo-Pacific region during the northern winter. *Climate Dynamics*, (1998), doi:10.1007/s00382-015-2528-y.



Nakamura, H., 1992: Midwinter Suppression of Baroclinic Wave Activity in the Pacific. *Journal of the Atmospheric Sciences*, **49 (17)**, 1629–1642, doi:10.1175/1520-0469(1992)049<1629:MSOBWA>2.0.CO;2.

Nakamura, H., 2002: Trapping of synoptic-scale disturbances into the North-Pacific subtropical jet core in midwinter. *Geophysical Research Letters*, **29 (16)**, 10–13, doi:10.1029/2002GL015535.

Oleson, K. W., and Coauthors, 2010: Technical Description of version 4.0 of the Community Land Model (CLM). *NCAR Technical Note*, 266.

Puma, M. J., and B. I. Cook, 2010: Effects of irrigation on global climate during the 20th century. *Journal of Geophysical Research: Atmospheres*, **115 (16)**, 1–15, doi:10.1029/2010JD014122.

Rodell, M., I. Velicogna, and J. S. Famiglietti, 2009: Satellite-based estimates of groundwater depletion in India. *Nature*, **460 (7258)**, 999–1002, doi:10.1038/nature08238.

Roy, S. S., R. Mahmood, D. Niyogi, M. Lei, S. a. Foster, K. G. Hubbard, E. Douglas, and R. Pielke, 2007: Impacts of the agricultural Green Revolution-induced land use changes

on air temperatures in India. *Journal of Geophysical Research: Atmospheres*, **112** (21), 1–13, doi:10.1029/2007JD008834.



Sacks, W. J., B. I. Cook, N. Buening, S. Levis, and J. H. Helkowski, 2009: Effects of global irrigation on the near-surface climate. *Climate Dynamics*, **33** (2-3), 159–175, doi:10.1007/s00382-008-0445-z.

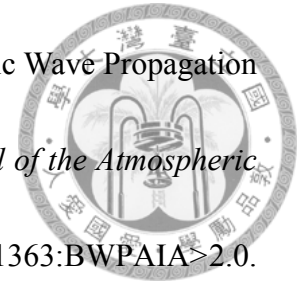
Saeed, F., S. Hagemann, and D. Jacob, 2009: Impact of irrigation on the South Asian summer monsoon. *Geophysical Research Letters*, **36** (20), 1–7, doi:10.1029/2009GL040625.

Saraf, A. K., A. K. Bora, J. Das, V. Rawat, K. Sharma, and S. K. Jain, 2011: Winter fog over the Indo-Gangetic Plains: Mapping and modelling using remote sensing and GIS. *Natural Hazards*, **58** (1), 199–220, doi:10.1007/s11069-010-9660-0.

Seneviratne, S. I., T. Corti, E. L. Davin, M. Hirschi, E. B. Jaeger, I. Lehner, B. Orlowsky, and A. J. Teuling, 2010: Investigating soil moisture-climate interactions in a changing climate: A review. *Earth-Science Reviews*, **99** (3-4), 125–161, doi:10.1016/j.earscirev.2010.02.004.

Shukla, S. P., M. J. Puma, and B. I. Cook, 2014: The response of the South Asian Summer Monsoon circulation to intensified irrigation in global climate model simulations. *Climate Dynamics*, **42** (1-2), 21–36, doi:10.1007/s00382-013-1786-9.

Simmons, a. J., J. M. Wallace, and G. W. Branstator, 1983: Barotropic Wave Propagation and Instability, and Atmospheric Teleconnection Patterns. *Journal of the Atmospheric Sciences*, **40 (6)**, 1363–1392, doi:10.1175/1520-0469(1983)040<1363:BWPAIA>2.0.CO;2.



Swann, a. L. S., I. Y. Fung, and J. C. H. Chiang, 2012: Mid-latitude afforestation shifts general circulation and tropical precipitation. *Proceedings of the National Academy of Sciences*, **109 (3)**, 712–716, doi:10.1073/pnas.1116706108.

Trenberth, K. E., G. W. Branstator, D. Karoly, A. Kumar, N.-C. Lau, and C. Ropelewski, 1998: Progress during TOGA in understanding and modeling global teleconnections associated with tropical sea surface temperatures. *Journal of Geophysical Research*, **103 (C7)**, 14 291, doi:10.1029/97JC01444.

UNEP, 2008: Vital water graphics – An overview of the state of the world’s fresh and marine waters – 2nd edition. Tech. rep. doi:92-807-2236-0, [92-807-2236-0](https://doi.org/10.1017/9781107329424).

Voss, K. a., J. S. Famiglietti, M. Lo, C. De Linage, M. Rodell, and S. C. Swenson, 2013: Groundwater depletion in the Middle East from GRACE with implications for trans-boundary water management in the Tigris-Euphrates-Western Iran region. *Water Resources Research*, **49 (2)**, 904–914, doi:10.1002/wrcr.20078.

Wallace, J. M., and D. S. Gutzler, 1981: Teleconnections in the Geopotential Height Field

during the Northern Hemisphere Winter. 784–812 pp., doi:10.1175/1520-0493(1981)109<0784:TITGHF>2.0.CO;2.



Wisser, D., S. Frohking, E. M. Douglas, B. M. Fekete, C. J. Vörösmarty, and A. H. Schumann, 2008: Global irrigation water demand: Variability and uncertainties arising from agricultural and climate data sets. *Geophysical Research Letters*, **35** (24), 1–5, doi:10.1029/2008GL035296.

Yao, T., and Coauthors, 2012: Different glacier status with atmospheric circulations in Tibetan Plateau and surroundings. *Nature Climate Change*, **2** (7), 1–5, doi:10.1038/nclimate1580.

Yasmeen, Z., G. Rasul, and M. Zahid, 2012: Impact of Aerosols on Winter Fog of Pakistan. *Pakistan Journal of Meteorology*, **8** (16), 21–30.

Yeh, T.-C., R. T. Wetherald, and S. Manabe, 1984: The Effect of Soil Moisture on the Short-Term Climate and Hydrology Change —A Numerical Experiment. *Monthly Weather Review*, **112** (3), 474–490, doi:10.1175/1520-0493(1984)112<0474:TEOSMO>2.0.CO;2.

Zhang, K., J. S. Kimball, R. R. Nemani, and S. W. Running, 2010: A continuous satellite-derived global record of land surface evapotranspiration from 1983 to 2006. *Water Resources Research*, **46** (9), 1–21, doi:10.1029/2009WR008800.



Tables

Table 2.1: Model setup

Case	Irrigation
CTR	No
IRR	Yes, climatological irrigation; the amount is 1991-2000 mean

Table 3.1: Simulated results averaged over IGP for different runs. Numbers in brackets are averaged over all India (0-40°N, 60-100°E)

	CTR	IRR	IRR-CTR
Top 10 cm soil water (kg/m ²)	21.01 (20.34)	23.88 (21.56)	2.87 (1.22)
Latent heat (W/m ²)	25.92 (46.53)	37.74 (50.67)	11.82 (4.14)
Low cloud cover (fraction)	2.46% (10.27%)	3.26% (12.00%)	0.80% (1.73%)
Surface downwelling solar radiation (W/m ²)	223.49 (213.53)	220.98 (210.46)	-2.51 (-3.07)
Reference height temperature (K)	285.79 (284.52)	284.82 (283.96)	-0.97 (-0.56)



Figures

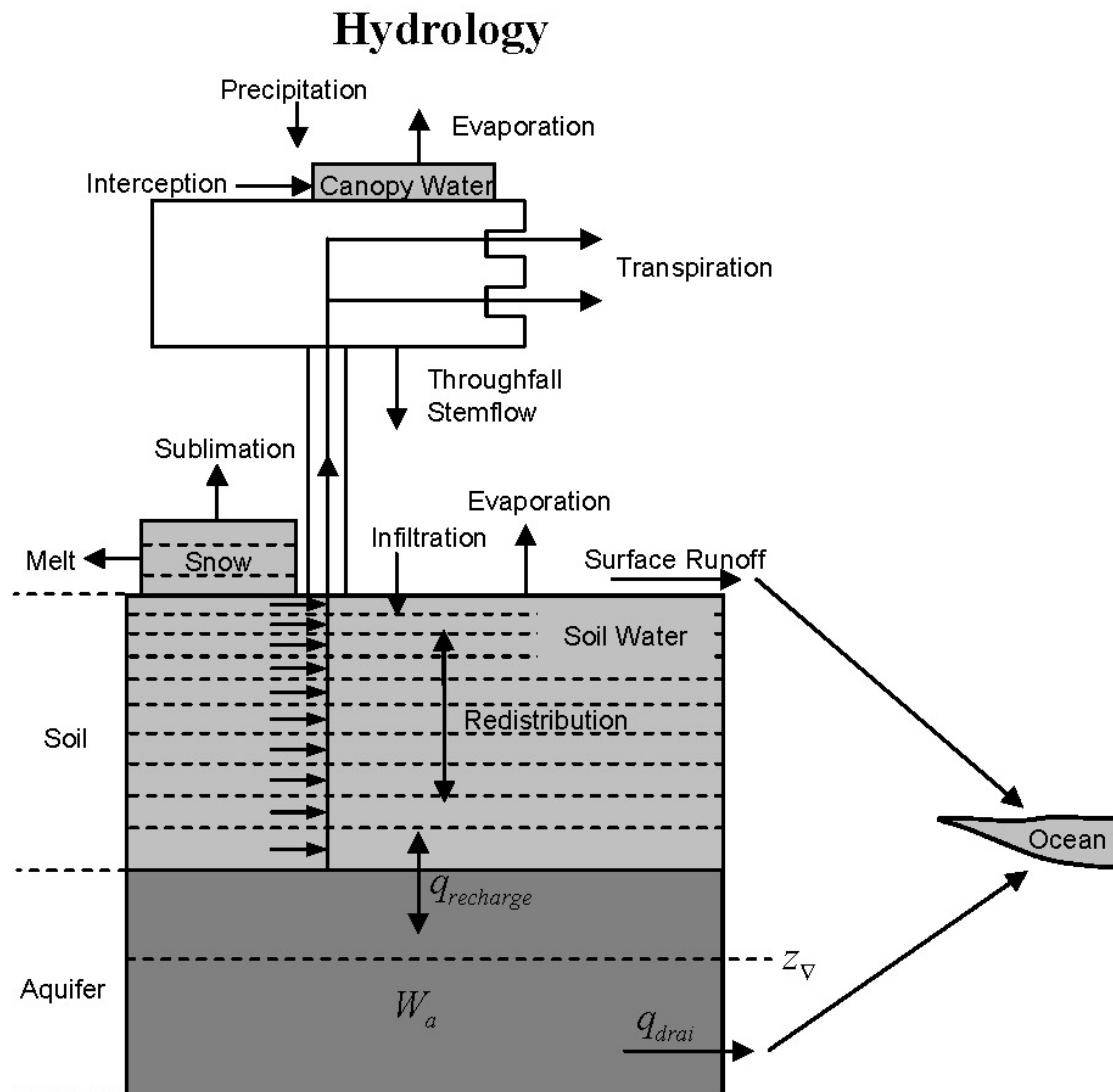


Figure 2.1: Hydrology processes simulated in CLM4. Taken from CLM4 tech note (Oleson et al., 2010).

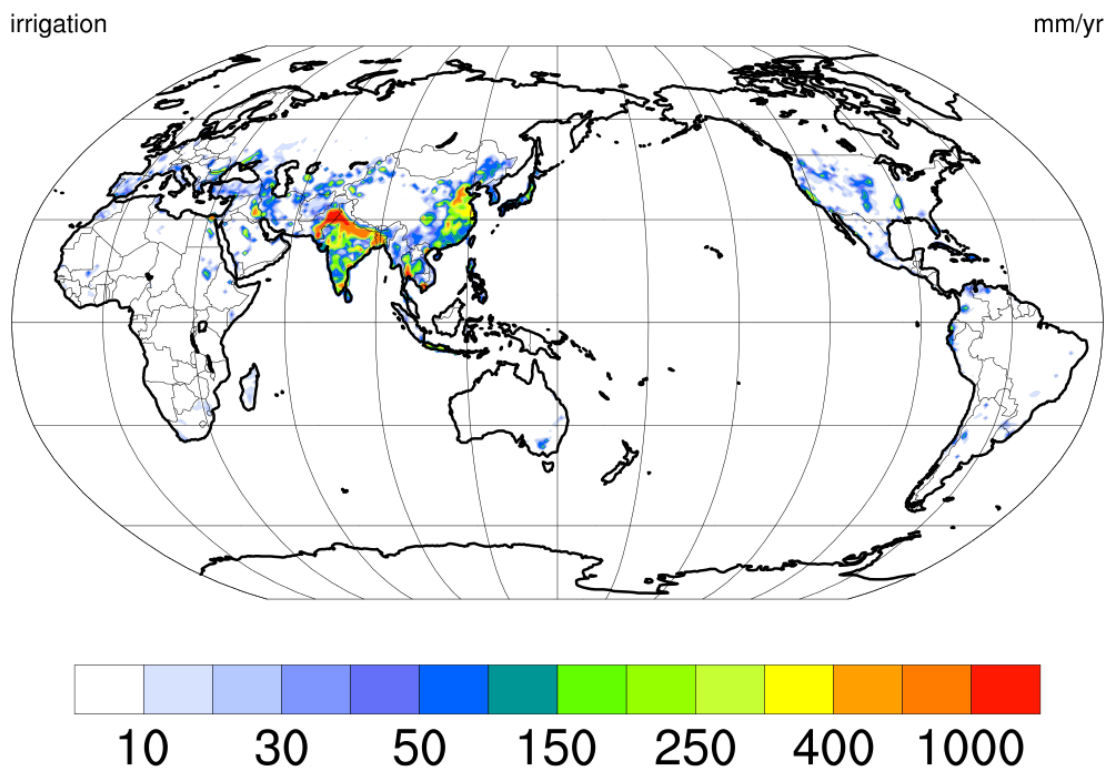


Figure 2.2: Global annual mean irrigation added in the simulation (mm/year)

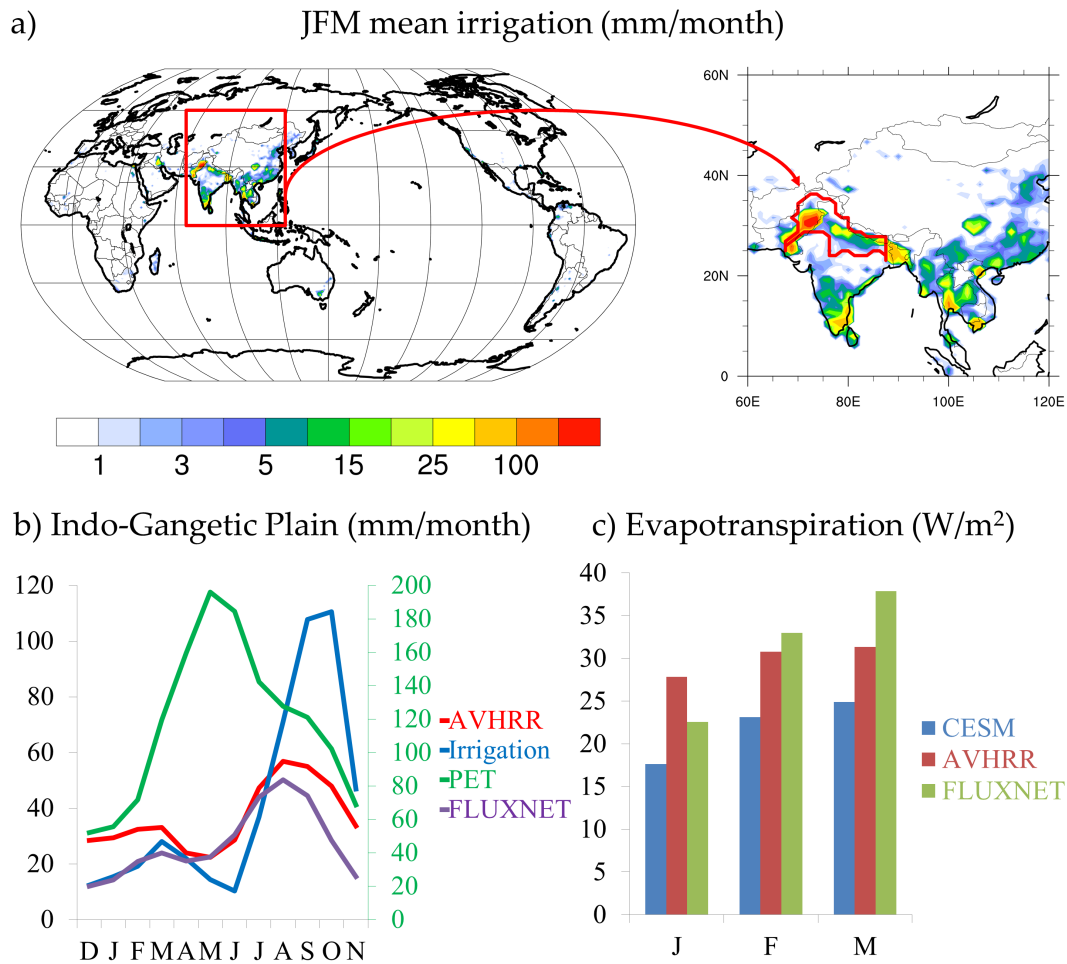


Figure 3.1: (a) January-March mean irrigation amount (mm/month). The location of IGP is also shown. (b) Climatological means of AVHRR and FLUXNET based ET, irrigation amount and PET averaged over IGP (mm/month). (c) Simulated IGP mean ET from CESM compared with the two observation products (W/m^2).

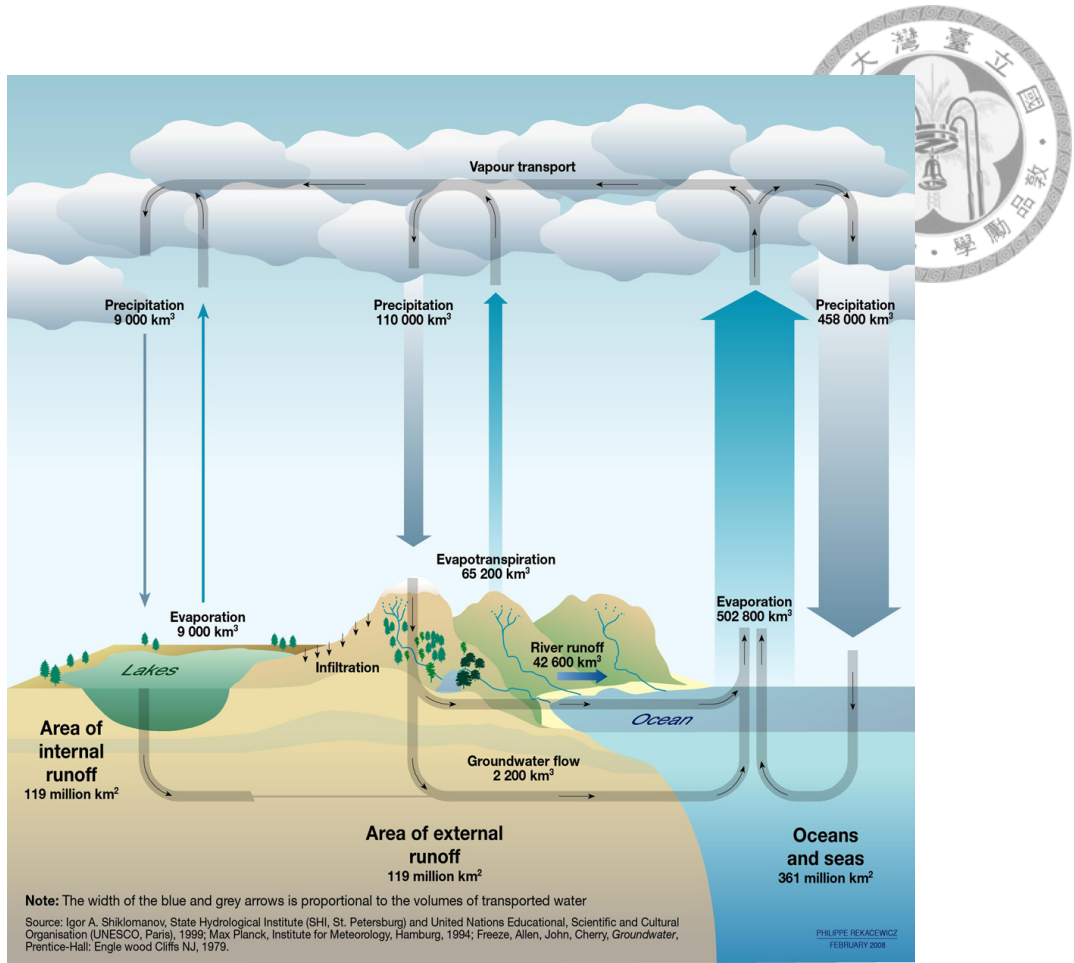


Figure 3.2: The water cycle. Taken from [UNEP \(2008\)](#)

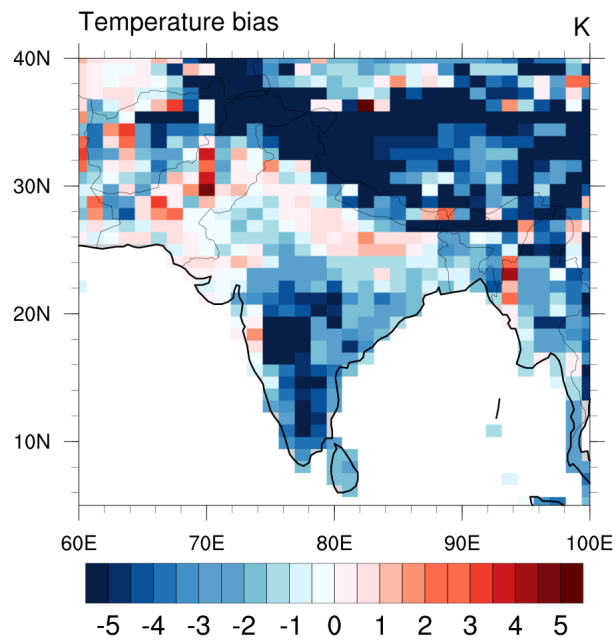


Figure 3.3: CESM temperature bias in JFM compared with CRU record (K)

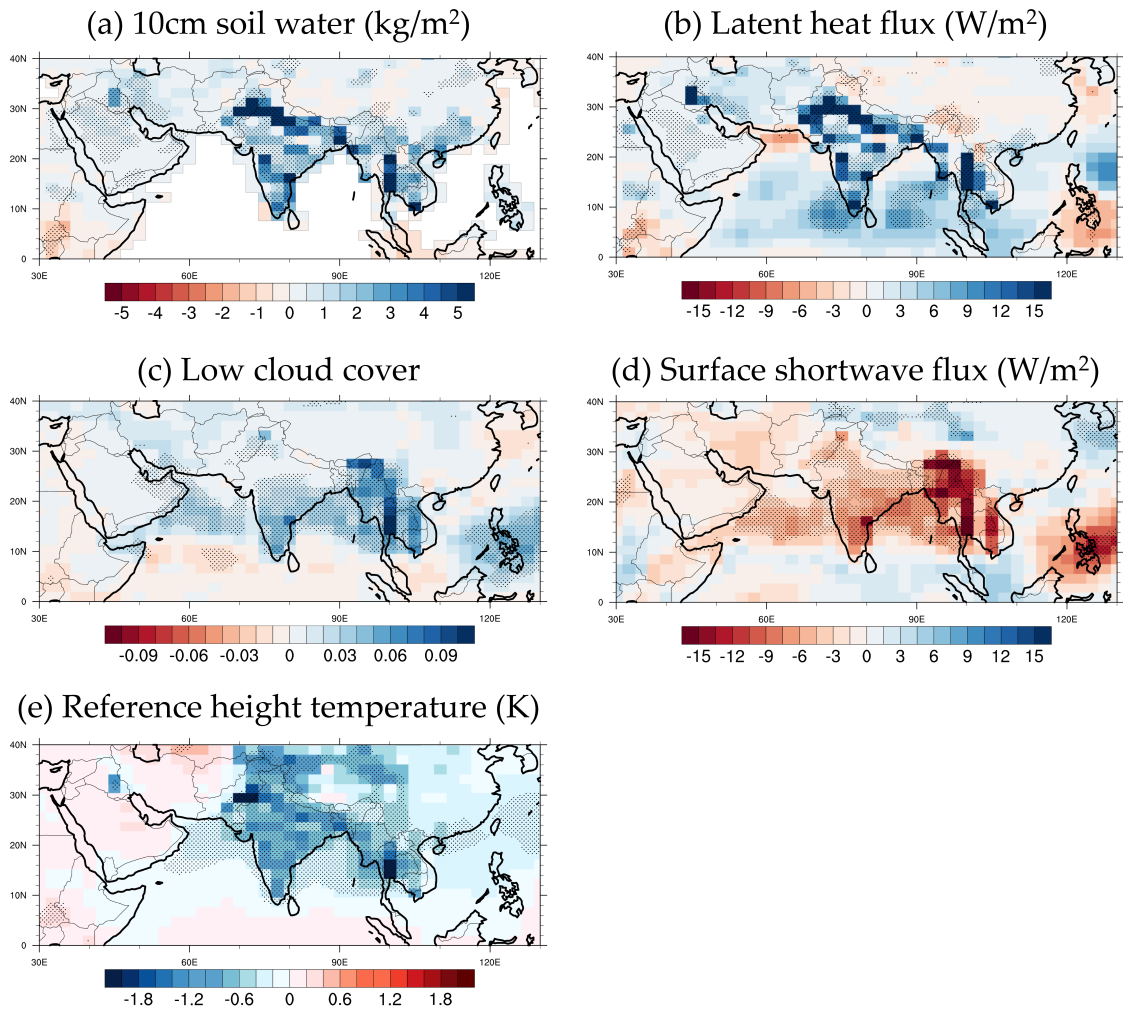
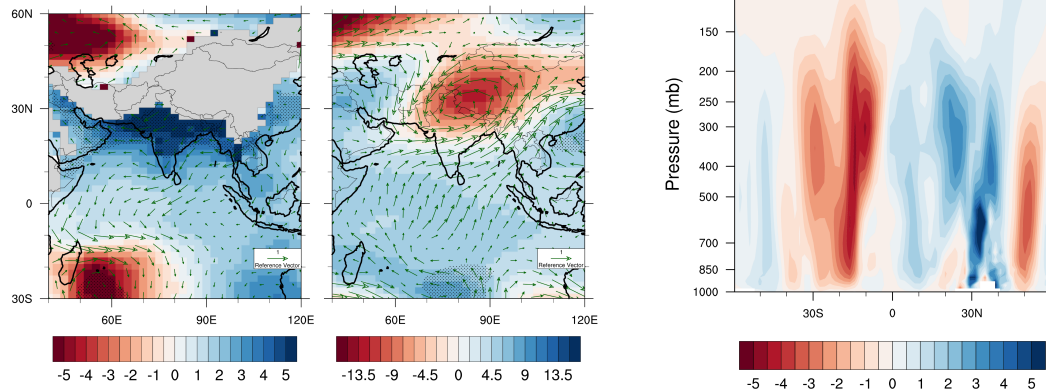


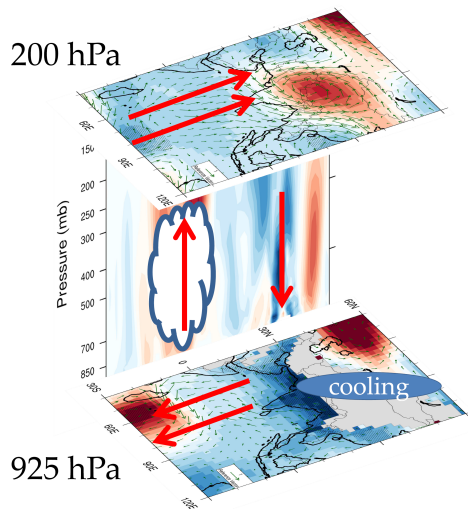
Figure 3.4: IRR-CTR (a) 10cm soil water (kg/m^2) (b) latent heat flux (W/m^2) (c) low cloud cover (d) surface downwelling shortwave flux (W/m^2) and (e) reference height temperature (K). (dotted: $p < 0.1$)



(a) 925 hPa and (b) 200 hPa Geopotential height (m) and wind (m/s) (c) 40E-90E Vertical velocity (10^{-3} Pa/s)



(d) Schematic diagram



(e) 200 hPa Velocity potential (10^5 m²/s)

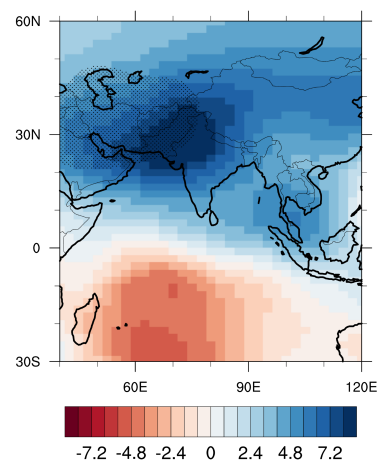


Figure 3.5: IRR-CTR (a) 925-hPa and (b) 200-hPa geopotential height (shading, m) and wind (vector, m/s) (c) 40E-90E mean vertical velocity (10^{-3} Pa/s) (d) Schematic diagram showing the process of which irrigation causes monsoon changes (e) IRR-CTR 200-hPa velocity potential (10^5 m²/s) (dotted: $p < 0.1$ for a, b, and e)

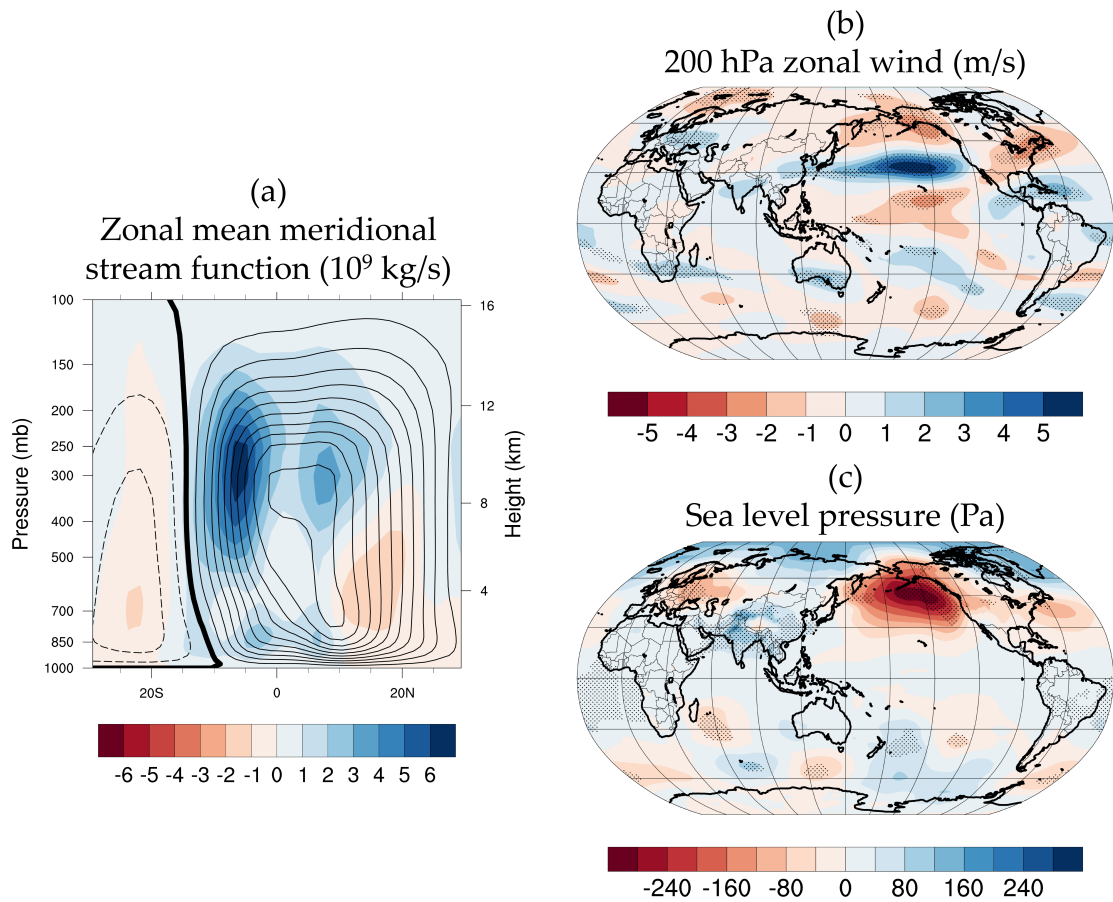


Figure 3.6: (a) zonal mean meridional stream function (shading: IRR-CTR, 10^9 kg/s; contour: CTR, CI: 0.2×10^{11} kg/s, positive (negative) values are in solid (dashed) lines) (b) IRR-CTR 200-hPa zonal wind (m/s) (c) IRR-CTR sea level pressure (Pa) (dotted: $p < 0.1$ for b and c)

Total (convective and large-scale) precipitation rate (liq + ice)

mm/day

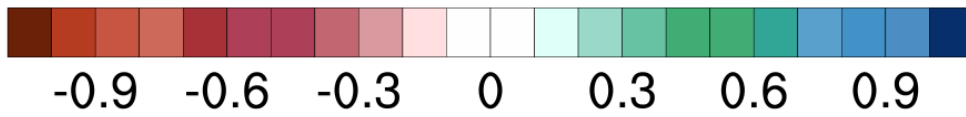
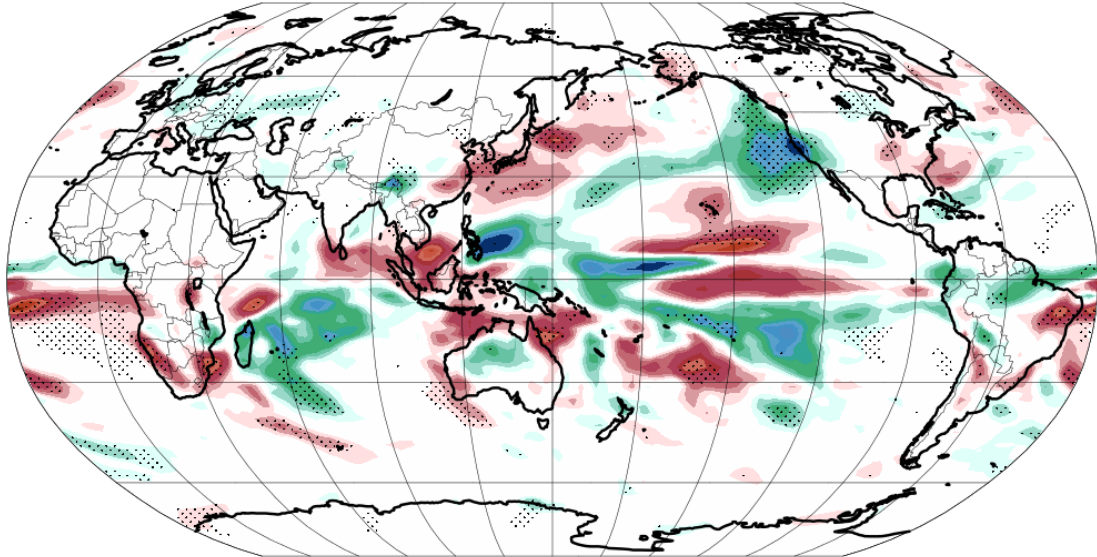


Figure 3.7: IRR-CTR total precipitation rate (mm/day) (dotted: $p < 0.1$)

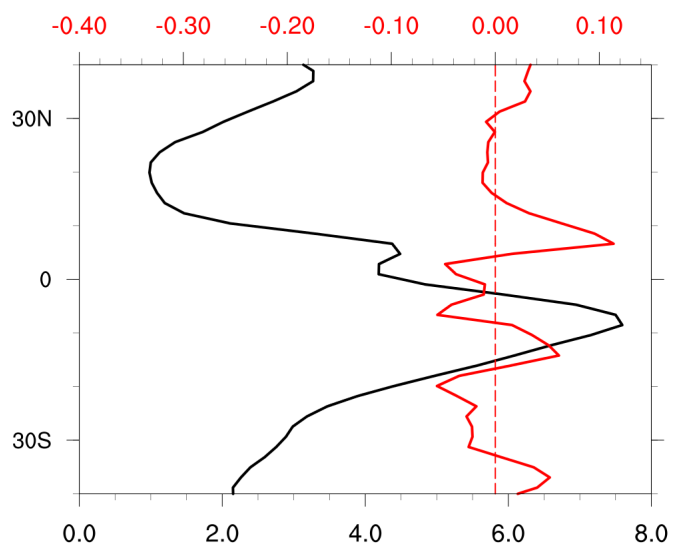


Figure 3.8: IRR-CTR (red) and CTR (black) zonal mean precipitation (mm/day)

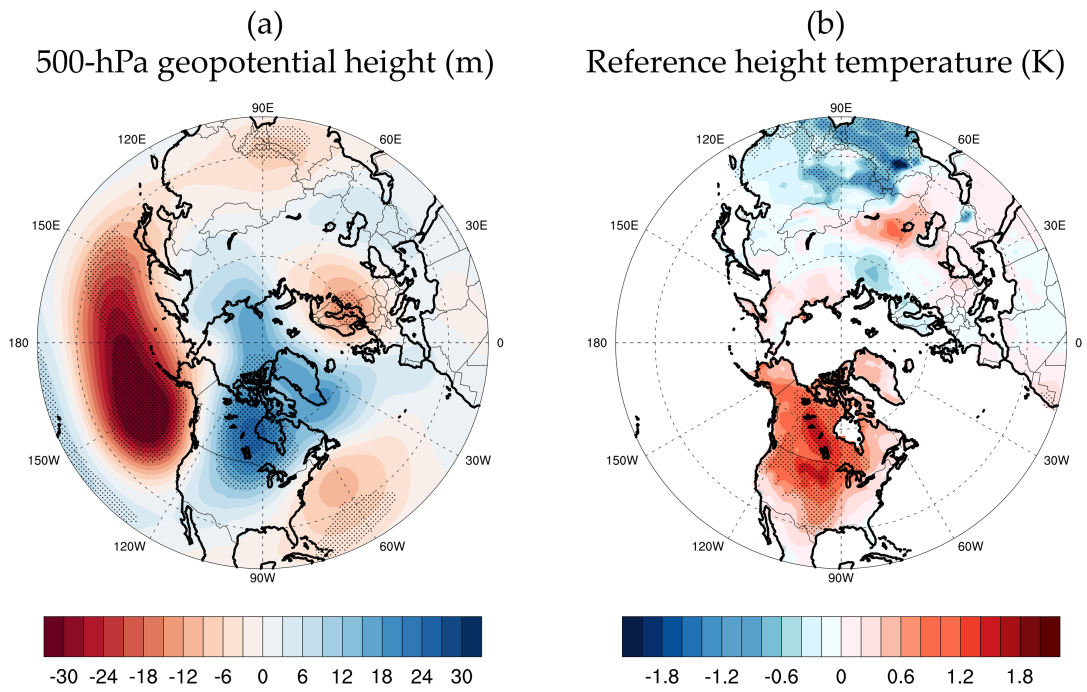


Figure 3.9: Differences (IRR-CTR) in (a) 500-hPa geopotential height (m); (b) reference height temperature over North America (K) (dotted: $p < 0.1$).

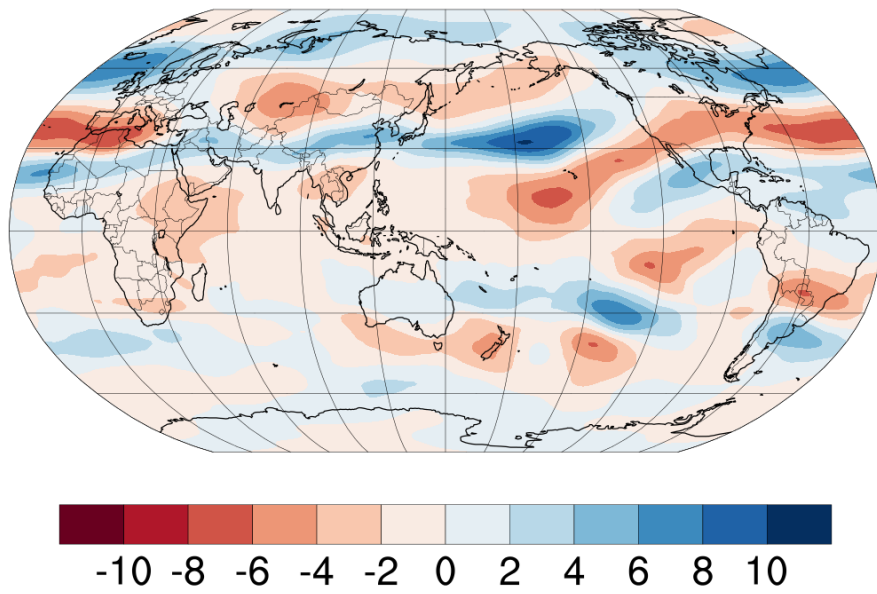
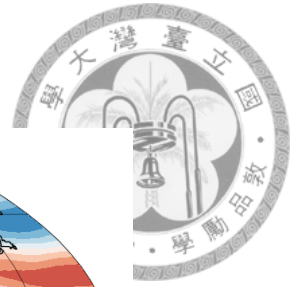


Figure 4.1: Composite 200-hPa zonal wind difference (ERA-Interim reanalysis) (m/s)

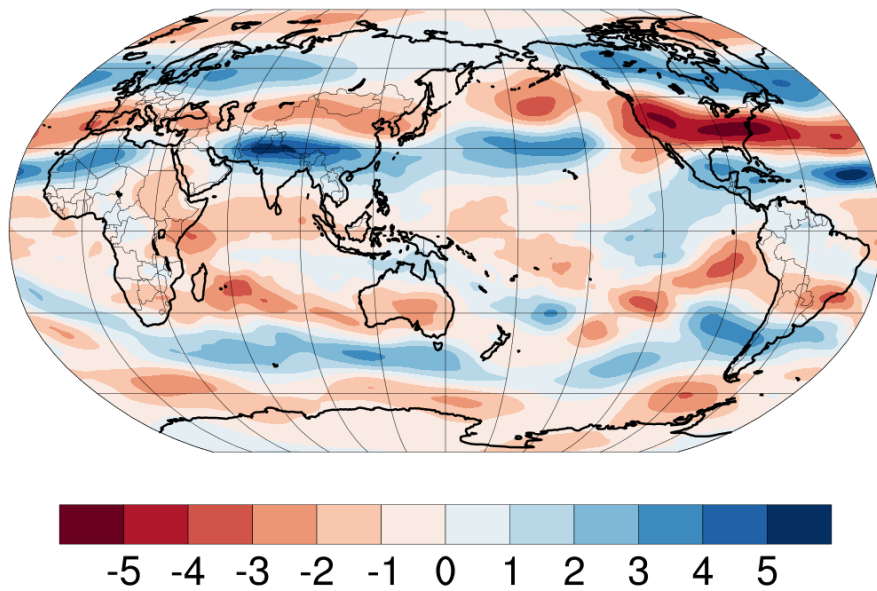


Figure 4.2: Composite 200-hPa zonal wind difference (Last Millennium simulation) (m/s)

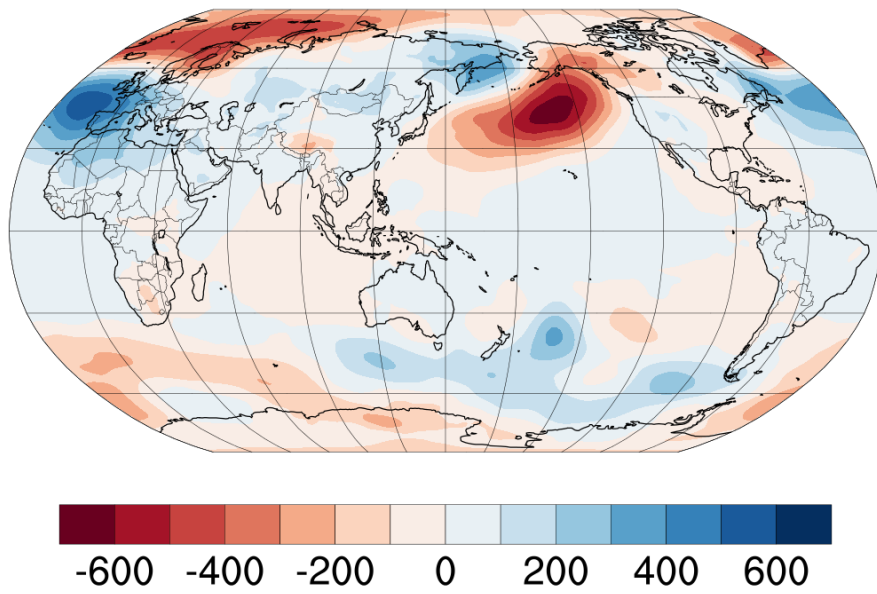
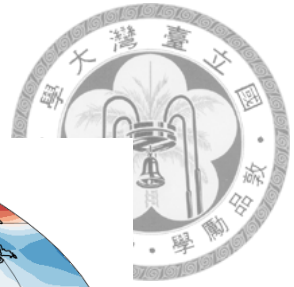


Figure 4.3: Composite sea level pressure difference (ERA-Interim reanalysis) (Pa)

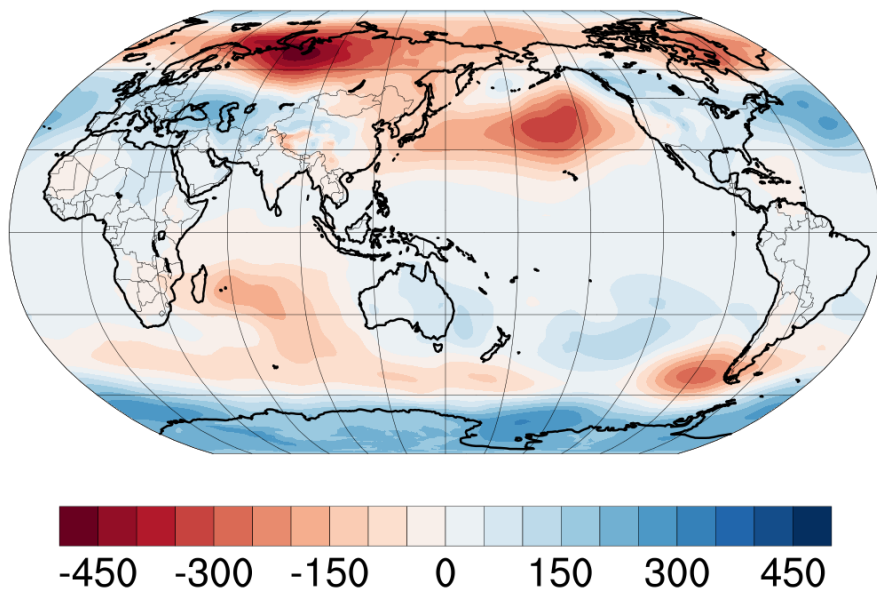


Figure 4.4: Composite sea level pressure difference (Last Millennium simulation) (Pa)

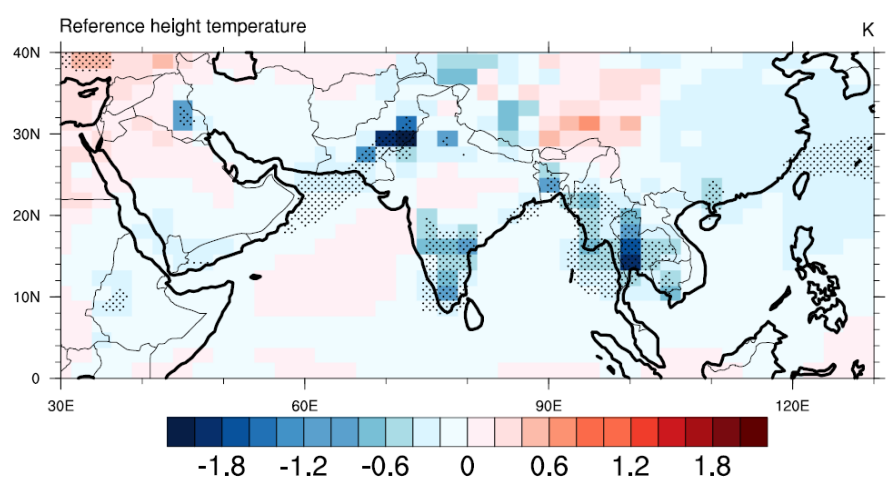
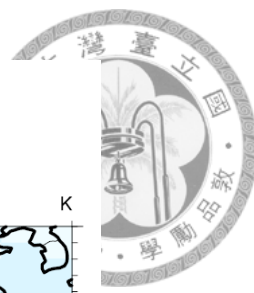


Figure 4.5: IrrDJFM-CTR reference height temperature (K) (dotted: $p < 0.1$)

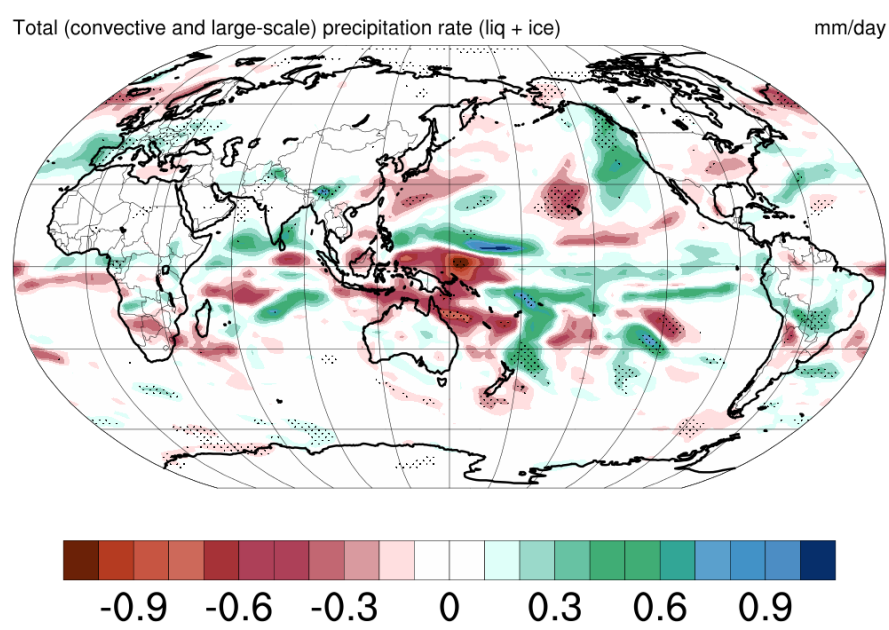
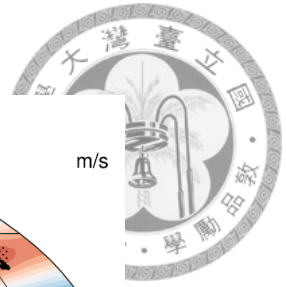


Figure 4.6: IrrDJFM-CTR total precipitation rate (mm/day) (dotted: $p < 0.1$)



Zonal wind

m/s

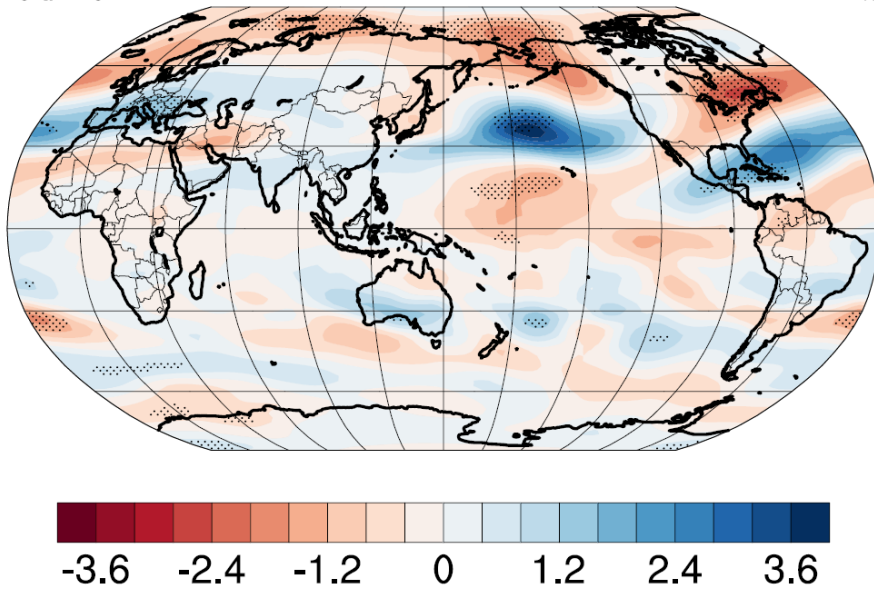


Figure 4.7: IrrDJFM-CTR 200-hPa zonal wind (m/s) (dotted: $p < 0.1$)

Sea level pressure

Pa

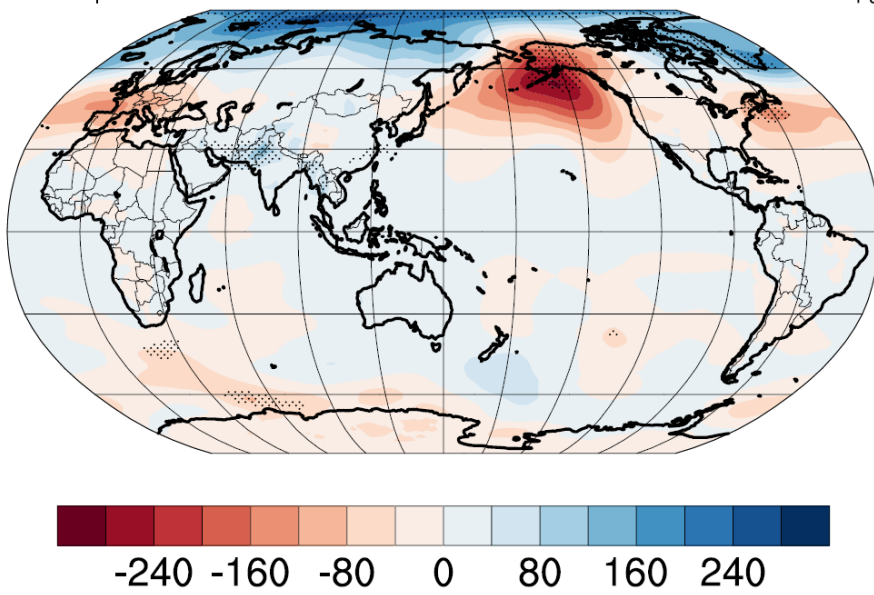


Figure 4.8: IrrDJFM-CTR sea level pressure (Pa) (dotted: $p < 0.1$)

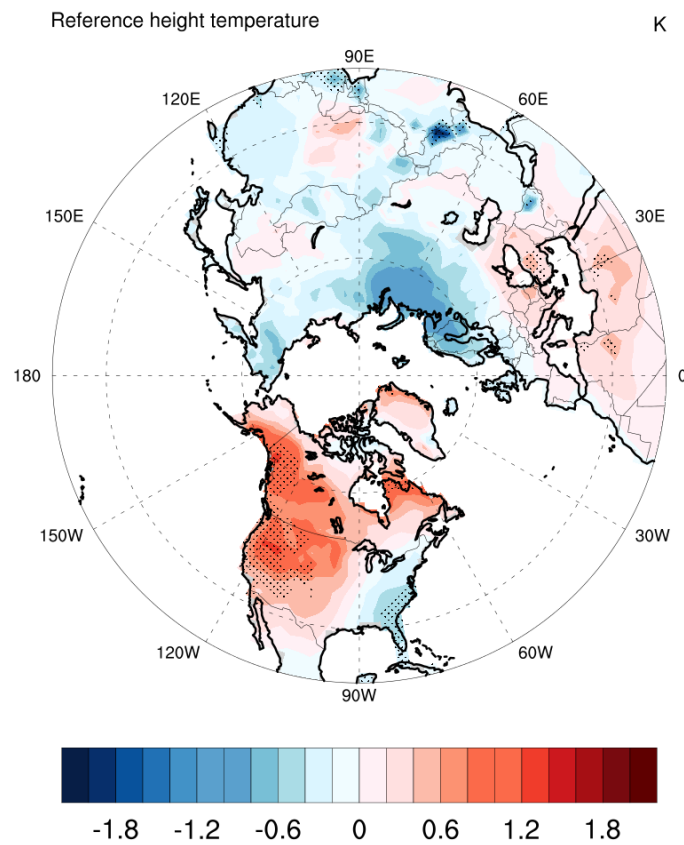


Figure 4.9: Differences (IrrDJFM-CTR) in reference height temperature over North America (K) (dotted: $p < 0.1$).

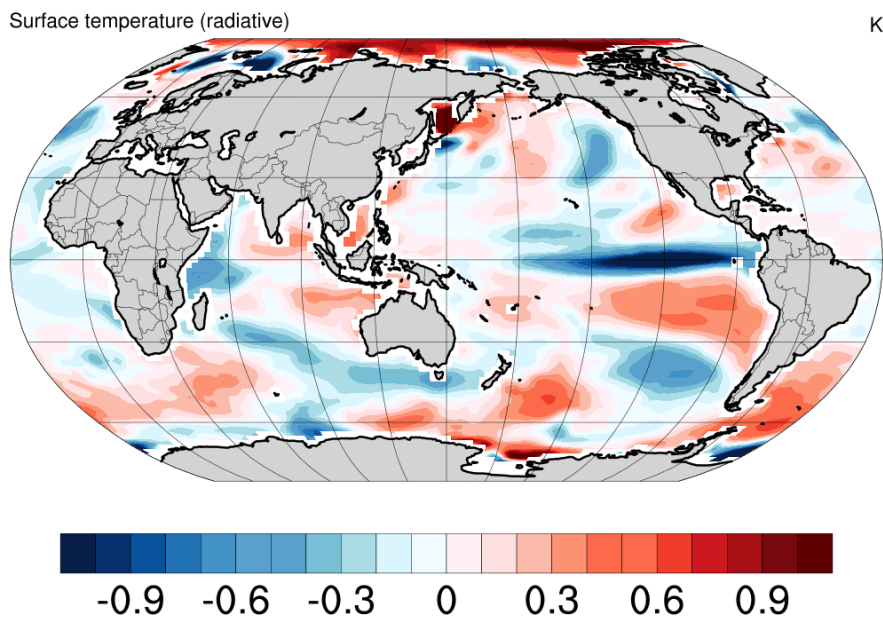


Figure 4.10: Differences (composite members-CTR) in SST globally (K).

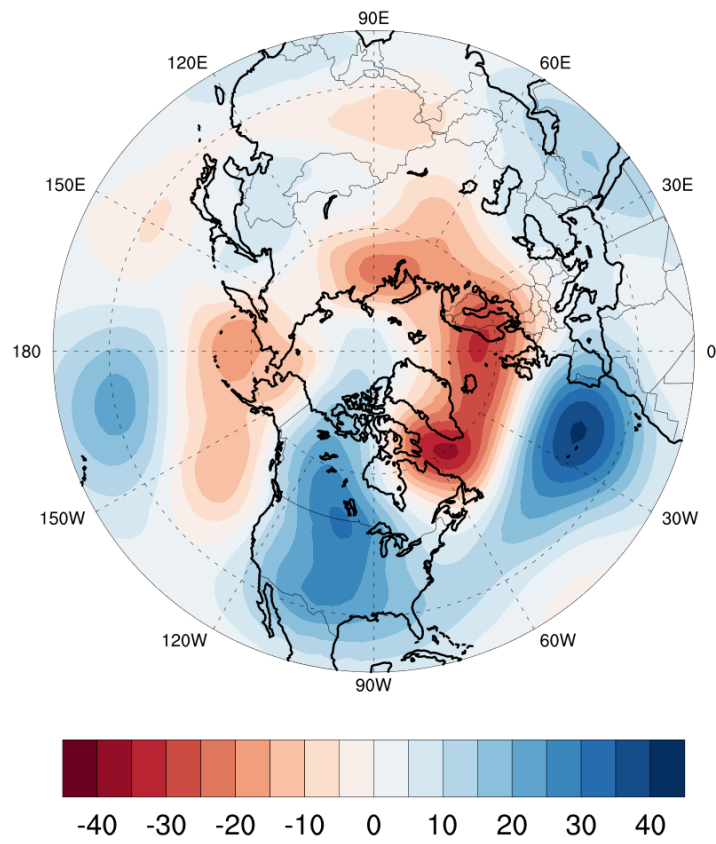


Figure 4.11: Differences (composite members-CTR) in 500-hPa geopotential height (m).

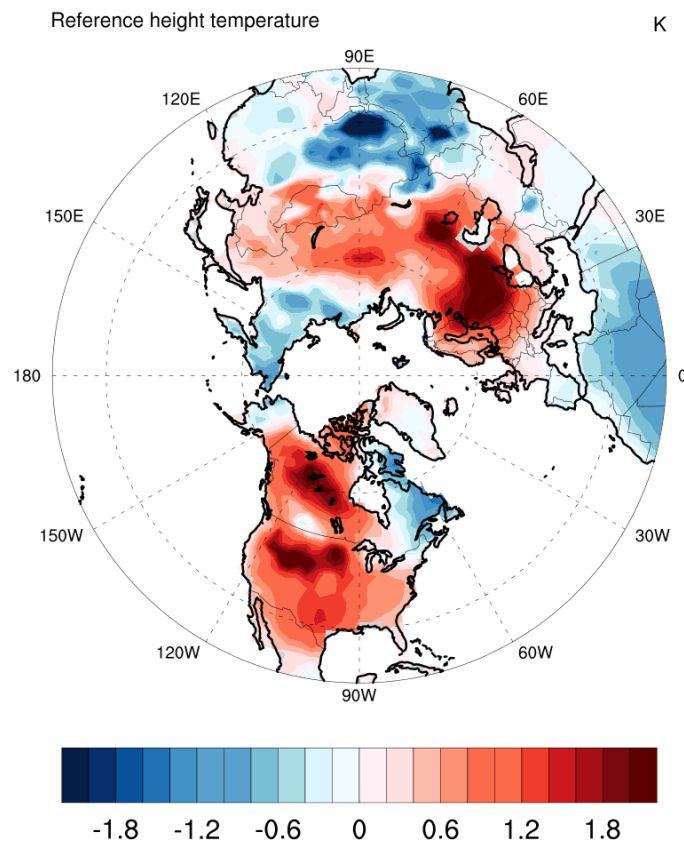


Figure 4.12: Differences (composite members-CTR) in reference height temperature(K).

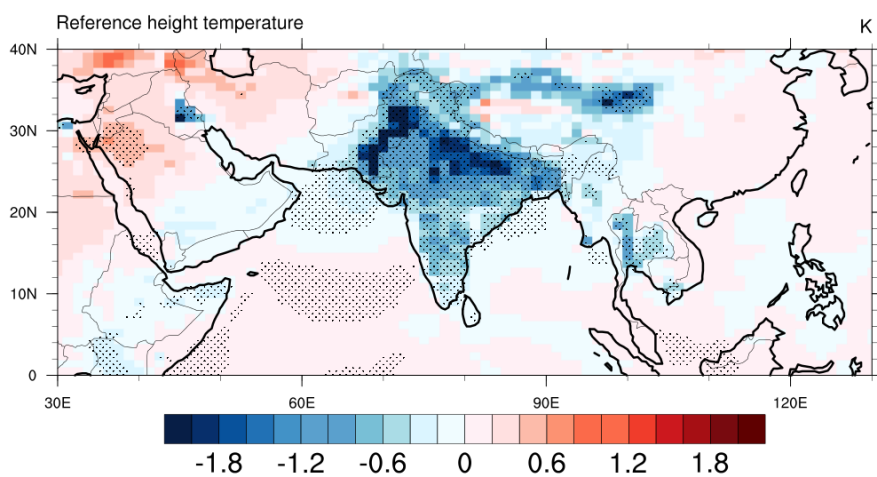


Figure 4.13: Differences (IrrAGCM-CtrAGCM) in reference height temperature over South Asia (K) (dotted: $p < 0.1$).

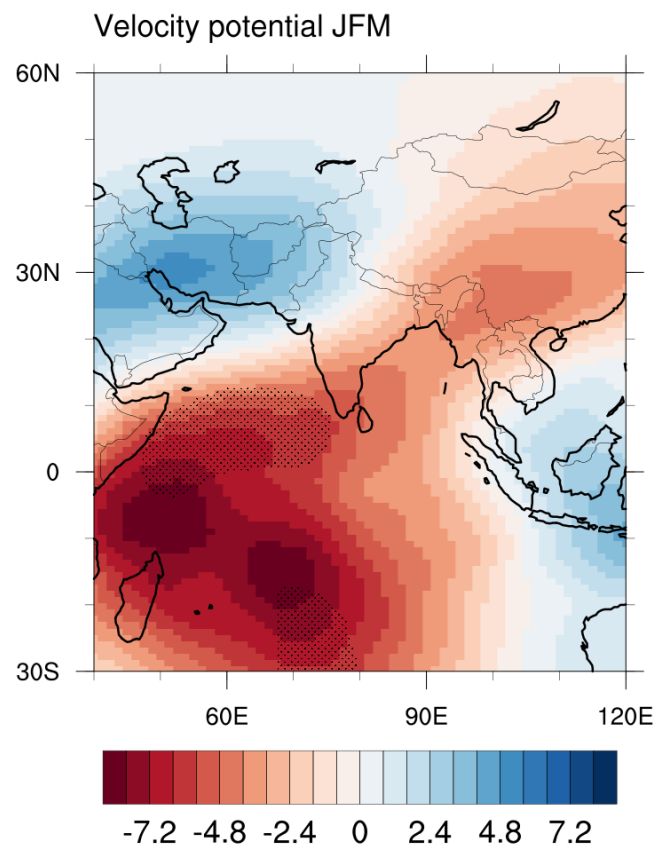


Figure 4.14: Differences (IrrAGCM-CtrAGCM) in 200-hPa velocity potential ($10^5 \text{ m}^2/\text{s}$) (dotted: $p < 0.1$)

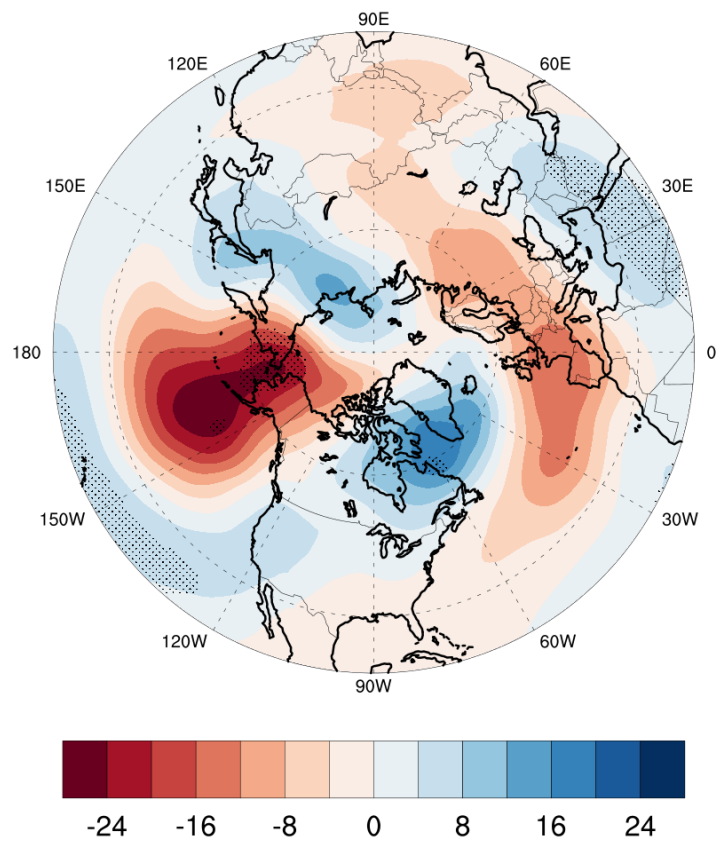


Figure 4.15: Differences (IrrAGCM-CtrAGCM) in 500-hPa geopotential height (m) (dotted: $p < 0.1$).

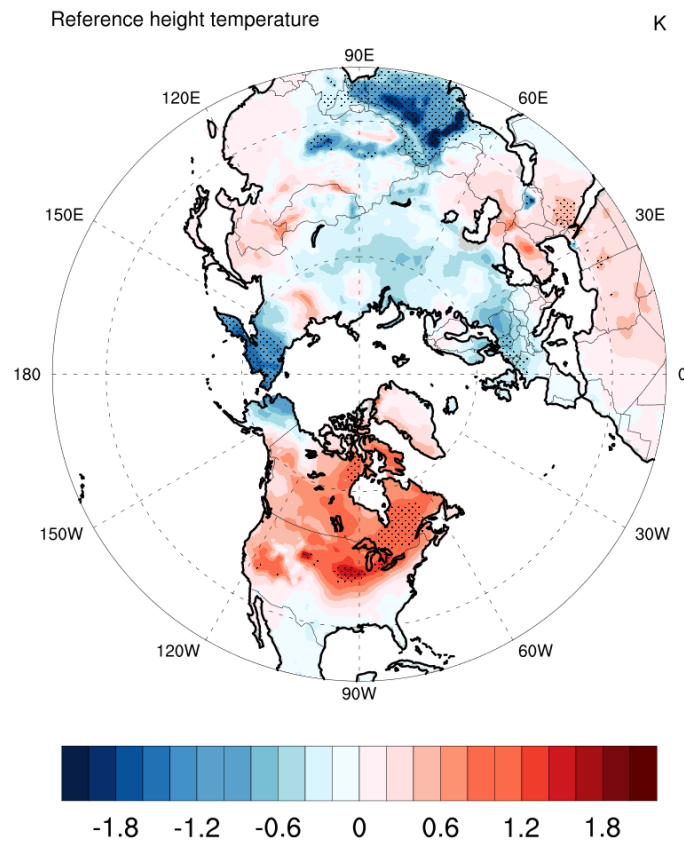


Figure 4.16: Differences (IrrAGCM-CtrAGCM) in reference height temperature over North America (K) (dotted: $p < 0.1$).

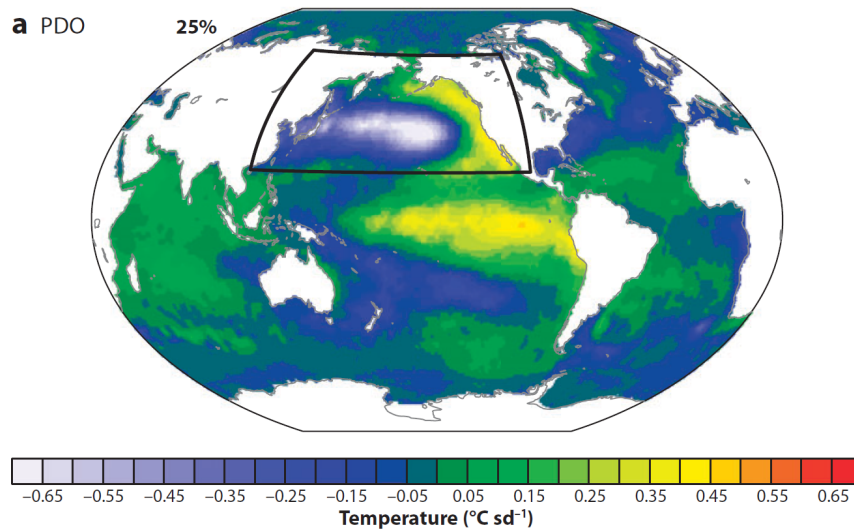


Figure 5.1: PDO pattern. Taken from [Deser et al. \(2010\)](#)